TALTECH

TALLINN UNIVERSITY OF TECHNOLOGY

SCHOOL OF ENGINEERING

Department of Mechatronics and Autonomous Systems

THESIS TITLE

WEARABLE BLUETOOTH MONITOR OF CARDIOVASCULAR DATA.

KARDIOVASKULAARSÜSTEEMI KANTAV BLUETOOTH MONITOR

MASTER THESIS

Üliõpilane:	Stephen Smart Japhet
	/nimi/
Üliõpilaskood:	185763MAHM
	Paul Annus (Senior Research Scientist)
	Marek Rist (Researcher)
Juhendaja:	Madis Ratassepp (Senior Research Fellow)
	/nimi, amet/

Tallinn 2021

AUTHOR'S DECLARATION

Hereby I declare, that I have written this thesis independently.

No academic degree has been applied for based on this material. All works, major viewpoints and data of the other authors used in this thesis have been referenced

"18" may 2021.

Student: Stephen Smart Japhet .... "18" May 2021

/signature/

Thesis is in accordance with terms and requirements

"18" May 2021

Supervisor: …..........................

/signature/

Accepted for defence

"18" may 2021.

Chairman of theses defence commission: ....

/name and signature/

Non-exclusive Licence for Publication and Reproduction of GraduationTthesis[1]

I, Stephen Smart Japhet (name of the author) (date of birth: 14/12/1991) hereby

1. grant Tallinn University of Technology (TalTech) a non-exclusive license for my thesis
Wearable Bluetooth Monitor of Cardiovascular Data,

(*Wearable Bluetooth Monitor of Cardiovascular Data*)

supervised by Paul Annus,

(*Supervisor's name*)

1.1 reproduced for the purposes of preservation and electronic publication, incl. to be entered in the digital collection of TalTech library until expiry of the term of copyright;

1.2 published via the web of TalTech, incl. to be entered in the digital collection of TalTech library until expiry of the term of copyright.

1.3 I am aware that the author also retains the rights specified in clause 1 of this license.

2. I confirm that granting the non-exclusive license does not infringe third persons' intellectual property rights, the rights arising from the Personal Data Protection Act or rights arising from other legislation.

---

[1] *Non-exclusive Licence for Publication and Reproduction of Graduation Thesis is not valid during the validity period of restriction on access, except the university`s right to reproduce the thesis only for preservation purposes.*

Student: Stephen Smart Japhet .... "18" May 2021

/signature/

Department of Mechatronics and Autonomous Systems

THESIS TASK

Student: Stephen Smart Japhet 186357MAHM (name, student code)

Study programme,   MAHM02/18 Mechatronics (code and title)

main speciality: Mechatronics

Supervisor(s): Paul Annus, Senior Research Scientist (position, name, phone)

Co-Supervisor: Marek Rist, Senior Research Fellow (name, position)

Co-Supervisor: Madis Ratassepp, (name, position)

……………………………………………………………………………… (company, phone, e-mail)

Thesis topic:

(in English)   _Wearable Bluetooth Monitor of Cardiovascular data_

(in Estonian) Kardiovaskulaarsüsteemi kantav Bluetooth monitor

Thesis main objectives:

- Porting the nRF8001 SDK Library from the Arduino platform to ARM Cortex M3.
- Writing program to process output data from the sensors and sending them to SPI0.
- Writing a handler to listen for new data on the SPI0.
- Configuring nRF8001 to connect to a phone via BLE.

Thesis tasks and time schedule:

No	Task description	Deadline
1.	Planning and review of system software and hardware datasheets	February 2021

2.	Hardware and Software Implementation and Prototype	March-May 2021
3.	Testing and drawing Conclusion	May 2021

Language: English **Deadline for submission of thesis:** "18" May 2021

Student: Stephen Smart Japhet .... "18" May 2021

/signature/

Supervisor: Paul Annus .... "18" May 2021

/signature/

Co-Supersor: Madis Ratassep …..................... "18" May 2021

/signature/

Head of study programme: .... "18" May 2021

/signature/

Terms of thesis closed defence and/or restricted access conditions to be formulated on the reverse side

TABLE OF CONTENTS

PREFACE

My sincere appreciation goes to God Almighty for giving me the strength and privilege to complete this thesis work successfully during this hard time of Covid-19. Without His grace, I will be lost.

To my supervisor, Paul Annus, thank you for your contributions and support towards the completion of this research work thesis. To my co-supervisors Marek Rist and Madis Ratassepp thank you for all the help and energy you put forward towards the completion of this thesis.

My special gratitude also goes to all my parents Stephen Bandawa, Beatrice Ali, Rev (Dr.), and Mrs. Nemuel Babba. To my sisters, Sandra and Hope Stephen, thank you for all yours prayers. To all my families, friends, and well-wishers, I say a big thank you all for the support all these years.

List of abbreviations and symbols

AC	Alternating Current
ACI	Application Controller Interface
AFE	Analog Front End
AHB	Advanced High Performance Bus
AMBA	Advanced Microcontroller Bus Architecture
BLE	Blebluetooth Low Energy
BP	Blood Pressure
CO	Cardiac Output
CVD	Cardiovascular Disease
DC	Direct Current
DFT	Discrete Fourier Transform
DMA	Direct Memory Access
DWT	Data Watchpoint And Trace
EBI	Electrical Bioimpedance
ECG	Electrocardiogram
EIM	Electrical Impedance Myography
EIT	Impedance Tomography
EKSP	Evaluation Kit Support Package
EMC	Electromagnetic Compatibility
EMG	Electromyography
EWARM	Embedded Workshops For ARM
FDA	Food and Drug Administration
FPC	Flexible Printed Circuits
HR	Pulse Rate
ICG	Impedance Cardiography
LA	Left Arm
LANs	Local-Area Networks
LL	Left Leg
MPU	Memory Protection Unit
MSPS	Megasamples Per Second
NFC	Near- Field Communication
NVIC	Nested Vectored Interrupt Controller
PCG	Phonocardiogram
PDA	Personal Digital Assistants
PLL	Phase-Locked Loop
PPG	Photoplethysmogram
RA	Right Arm
RR	Respiratory Rate
SAR	Sucessive Aproximation Register
SDK	Software Development Kit
SPI	Serial Peripheral Interface
SPO2	Blood Oxygen Saturation
SRAM	Static Random-Access Memory

List of figures

List of tables

1 INTRODUCTION

Healthcare is one of the fastest-growing business fields, and it is an important market for most countries. Healthcare services are the most needed and consumed service by mostly aging people around the world [1]. According to the U.S. Food and Drug Administration (FDA), they say that home healthcare is the fastest-growing segment of the medical device industry [2]. The surge in the medical device industry, which is caused by the increase by the number of people with chronic medical conditions, and rising health costs are some of the factors behind this trend. Wearable healthcare monitoring devices are attracting patients and doctors. Wearable devices will help to reduce the number of hospitalizations by providing the required healthcare services for patients at home and detention of emergencies, most especially among the elderly population suffering from chronic diseases.

As the saying goes, „with a healthy heart, the beat goes on" a healthy heartbeat is a good indicator of overall well-being. Our body needs a functioning heart to pump blood effectively and to supply vital oxygen and nutrients. Compromised heart health can lead to unforeseen complications and even death. A report by the American Heart Association's 2017 heart disease and stroke statistics update, an estimated 92.1 million adults in the U.S live with at least one type of cardiovascular disease, and the numbers are forecast to grow to 44% of the U.S population that is predicted to have some form of cardiovascular disease by the year 2030 [3], [4]. Cardiovascular disease (CVD) does harm to a person's health, and most concerns are with arrhythmia which is the leading cause of death. Cardiac arrhythmia is defined as abnormal heart rhythms, is a common type of CVD and, is thought to be responsible for most of the sudden cardiac deaths that occur every year [4], [5]. During a heart attack, the heart muscle is deprived of oxygen and the first few hours are critical in saving the patient. One of the delays in medical treatment is sometimes the lack of early warning and patient unawareness. Cardiovascular diseases have continued to be a problem in the medical field, and innovations in monitoring and management of cardiac patients are needed [3]. The Evolution of technologies has made it possible to collect and analyze the variety of vital physiological data with clinical usages, with an interface that is familiar and comfortable to the user. Medical wearable technologies are rising to this challenge.

The most common test for cardiac arrhythmia is an electrocardiogram (ECG). The ECG measures the electrical impulses of the heart via electrodes that are attached to the skin surface. Furthermore, diagnosing many arrhythmias with a standard resting ECG is difficult because it can only provide a snapshot of the patient's cardiovascular activity

in time. An intermittent arrhythmia can go far unnoticed, and physicians most times, must rely on self-monitoring and symptoms that are reported by patients to support their final diagnosis [5].

The human body has different physiological signs that can be measured ranging, from electrical signs to biochemical. It is possible to extract the human biosignals that can be analyzed to better understand our body health status and other reactions to external factors [6]. Some of the vital signs that have major importance to be measured are heart rate, blood oxygen saturation(SPO_2), blood pressure, respiratory rate, skin perspiration, and body temperature. Electrocardiography has good importance in heart-related electrical analysis. It is an important tool to predict and diagnose cardiovascular diseases Electrical bioimpedance (EBI) is a technique that includes delivering a tiny amount of electrical current through a volume of biological tissue and measuring the voltage change across that tissue to determine the passive resistance imposed against electrical current flow" [7].

Impedance is the measure of the opposition that a circuit presents to a current when a voltage is applied. Impedance was introduced by Oliver Heaviside in July 1886 [7] followed shortly after with admittance, which is the inverse of the impedance. Immittance is the combined term for impedance and admittance. Bioimpedance, therefore, is the measure of the opposition that a biological matter presents to a current when a voltage is applied.

The majority of wearable healthcare devices are designed with Bluetooth Low Energy (BLE) communication protocol, for physiological sign measurements and data gathering[1]. BLE is ideal for such applications because it requires a periodic transfer of data that can be analyzed. BLE is well suited for sensors devices and other low power consumption devices [1].

To accomplish the tasks of this thesis, an embedded firmware software program is developed for ADuCM350. The ADuCM350 is program to communicate with the nRF8001 Bluetooth for data transfer and the Bluetooth can send the received data to a mobile phone through UART.

1.1 Problem Statement

Many reports have suggested that the number of fatalities resulting from cardiovascular diseases will increase in the coming years globally. Cardiovascular disease is a major concern for the medical community and new innovations are needed for the monitoring

and management of cardiac patients. Furthermore, the symptoms in cardiovascular disease differ, and lack of early warning and patient unawareness are the most common causes of important delays in medical care. It is possible to predict the start of a heart attack and avoid patient error.

In this thesis, a wristwatch-like wearable Bluetooth device for monitoring and collecting data of physiological signs such as an electrocardiogram (ECG), heart rate, and blood oxygen saturation (SPO_2) has been proposed and developed. The data collected from this wearable device will be sent over Bluetooth to a different system (smartphone) that is later analyzed. All required hardware is assembled, and the embedded software of this device is programmed and tested.

Given the above challenges, this thesis seeks to answer the following:

The task of this thesis is to develop the embedded firmware driver for the NRF8001 module and the impedance based peripherals of the ADUCM350 microcontroller. The ADUCM350 has low user base and less resources, hence, increases the complexity of the project. Our goal is to create a prototype based on the custom embedded firmware to be developed utilizing the onboard impedance measuring peripheral and the other physiological signals based sensorics onbaord.

This list is a breakdown of the task to be acommplished.

- Write the driver code for the NRF8001 Bluetooth low energy module by porting the nRF8001 SDK Library from the Arduino platform to ARM cortex M3 of the ADUCM50 microcontroller.
- Write the driver code for the onboard impedance measuring peripheral and the vital signs sensors.
- Write the high-level abstraction code (main function) that utilizes the embedded firmware drivers developed. The main program extracts data from the sensors (ECG and SPO_2), processes the data, initializes the Bluetooth for data communication with receiving end.

1.2 Aims and Objectives

The aim of this thesis is to develop a wrist watch based smart wearable (WristIMP2) health monitoring prototype utilizing a custom embedded firmware driver on the ADUCM350 custom development board. The goal is to develop the embedded firmware drivers that the health monitoring appliction can use to gather data form the sensors (ECG and SPO_2), process the data and send the processd data over the bluetooth low energy module (NRF8001).

1.3 Methodology

An embedded firmware software program is developed for the custom made development board ADuCM350. The ADuCM350 is interface with nRF8001 Bluetooth over UART and the data received is send to a mobile phone for analysis.

The WristIMP2 (wristwatch-like) device is an implementation of ADUCM350, which is an integrated impedance measurement system that consists of ARM cortex M3, analog front-end and multiplexer, DDS for signal generation, 16bit ADC, and DFT engine. The ADUCM350 SDK is made for IAR embedded workshops. Additional components present are external 14bit dual-channel ADC (ADS7946) is connected through SPI1 and measures ECG voltage and battery voltage. The movement of the wrist and measurement device could be measured using ICM-20948. IMU also connects to the MCU over SPI1. SPI1 uses for data transfer between MCU and external 256Mb flash memory for storing measurement data.

The user interface consists of an RGB LED for indication of the state of the measurement device and displaying of battery-related notifications. The user input is a single push button that should wake up the device and put it into low power mode. The button is connected to hardware reset circuitry, and the 10s long-press causes a reset to the MCU. The measurement device has also optical heart rate and SPO2 sensor MAX30101EFD+ that is connected to the MCU through I2C and has a separate interrupt GPIO. The communication between the measurement device and host is over BLE. The device uses Nordic Semiconductors NRF8001 BLE.

1.4 Thesis Organisation

This thesis contains 5 chapters. Each chapter is structured as follows.

The first chapter of this thesis covers the introduction, problem statement, aims and objectives, methodology, and thesis organisation. The chapter two describes, the background and state of the art of wearable monirtoring devices. It goes further to discuss the vital signs in detail, and questions such as why do we measure them? What do we do with the measured data?, and the benefits of the measured data in medical piont view were answered. Furthermore, topics like impedance, bioimpedance and electrical bioimpedance (EBI) is discussed and the necessery questions were also answered. Finally, diagnostic tools such as electrocardiography (ECG) and photoplethysmogram (PPG) were discussed.

In chapter three, system on chip is discussed. The components of the hardware and software design were analyzed, and specifications given. The reasons for the chip selection and why the developmental board (microcontroller) is seclected for the project.

Chapter four covers the detailed description, of the hardware and software implementation. In chapter five, it contains the summary of the activities carried out in the thesis, and finally the conclusion drawn based on the results and many problems that I encounter during the embedded software development. The later part of this chapter outlines the recommended future work.

2 Background and State-of-the-Art of Wearable Devies

In this chapter, a background of wearable devices, physiological signs and overview of impedance bioimpedance, electrical bioimpedance, ECG were discussed.

2.1 Overview of Wearable Monitoring Devices

Wearable monitoring devices are referred to any electronic device that can be worn on the body, it can be informed of clothing, or accessory and have the ability to collect and transmit data that provides valuable insights related to the user's activities. Numerous wearable devices have been introduced over the years for monitoring biometric signals and other physiological signs. Some, examples such as the fitness trackers, were developed just for monitoring simple biologic features like physical activity and quality of sleep. Nowadays, the functions of wearables devices are not limited to such simple tasks [8]. The recent technological advancement in the medical field has made it practicable to collect and analyze different types of physiological data with clinical usages. These physiological signs include body temperature, respiratory rate, SPO_2 and heart rate.

Wearable devices can be sub-divided into two types the non-implantable and implantable devices. Non-implantable recording devices are those sensing electrode that is attached to the patient's body surface usually the chest, arms or wrist, which are suitable for short term recording and are very common. While the implantable devices are those that might require surgical operation to be inserted into the body [9].

Monitoring of the heart is one of the key challenges among health care professions [1]. With the advancement in technological development, this has help removed most of the hurdles in clinical application of wearable devices. These include the reduction of device size such as sensors, microprocessors and others, improved energy efficiency, and a patient friendly interface. These technological advancement have lead to many ground breaking archievements including in ECG measurements. Here are some possible three types of ECG solutions, (1) those that gather and store information, and later to be diagnosed in offline mode when the data collection is completed. (2) We have those that uses remote connectivity such as bluetooth, mobile phones or personal digital assistants (PDAs) to collect the ECG data, and to provide real-time diagnosis to an external server or monitoring center, where analysis and classification are performed. and finally (3) those that are build-in to perform real-time diagnosis within the device and display the results on screen. Example of offline systems include Holter monitors and event

recorders are well known names, like GE's SEER (GE Healthcare, Waukesha, WI), Philips's DigiTrack (Philips Healthcare, Andover, MA), and Midmark's IQmark (Midmark Corporation, Versailles, OH), to name a few. The mentioned devices can only provide recording, and monitoring capabilities but not real-time analysis because it is performed offline. Furthermore, the second type applies „telemedical" functionalities, meaning data is send to a remote rela-time monitoring system through phones or Bluetooth, where analysis are performed. And for the third type, researchers have proposed some intermediate level of local real-time classification over the years. Example of such as the classification include, heart beats, by using just smartphones but these do not provide a complete cardiovascular disease diagnosis solution [5].

There are numerous biometric signals that are use to determine heart rate and other regularities. The photoplethysmogram (PPG) is one of the widely used techniques for heart rhythm monitoring, and it also provides a simple, and other method for detection of arrhythmia. „The infrared light emitting source and a photodetector are the two major components of the device. PPG measure changes in blood volume in capillary blood vessels beneath the skin caused by the systolic and diastolic phases of the cardiac cycle." [8].
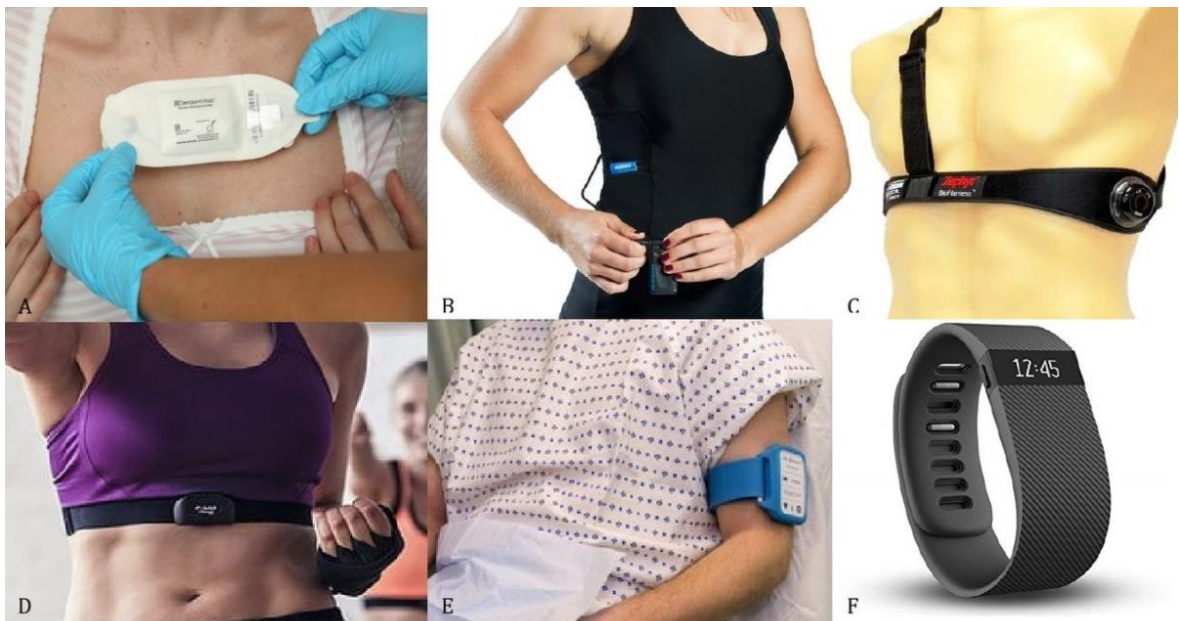
Figure 1. Examples of outpatient monitoring devices. (A) Medical Grade Adhesive Patch: from Sensium, Abingdon, UK. (B) Clothing with embedded sensors: from Hexoskin, Montreal, Canada. (C) Chest strap: from Medtronic, Maryland, USA. (D) Chest strap: from Polar Electro, Warwick, UK. (E) Upper armband: from Current, Edinburgh, UK. (F) Wristband: from Fitbit, San Francisco, USA [10].

As it is illustrated in figure 1 above, wearable monitoring devices can be grouped into many types such as patch monitors, clothing monitors, chest strap monitors, upper arm band monitors and wristband. Wristbands are by far the most common type of device currently and it is the focus of this thesis.

New features have been introduced in wearable devices to the users, as shown in figure 1 above. It is to help boost usability, convenience, and comfort to all users. The application of medical wearable devices consists of several steps, for example in cardiac monitoring devicess some steps include first, these wearable devices, are introduced to the user in the form of a wristwatch, clothing, chest strap, or other forms. When the user applied the device according to the instructions, the sensor of the wearable devices measures the specified parameters. Some of the useful data include electrocardiogram (ECG), heart rate, blood pressure, and others. The data collected is then transferred from the front-end sensor into a processed form that can be displayed to the user. The data is sent in a form of an electronic health record, with an app, or to a cloud-based server. The manufacturing of wearable devices is mainly dominanted by companies such as Fitbit, Xiaomi, Apple, and few others [3].

Much research has been carried out to improve the accuracy of signal monitoring, diagnosis, and user comfort in wearable devices. Improvement on materials, power consumption, life-cycle, size, and wearing parts for wearable devices have been made [9].

Tabel 1 Comparation for flexible sensors for vital sign monitoring [9].

	Vital Signs	Materials	Key Features	Limitations
Contact sensor	ECG/EMG	Ag NW/PDMS	Anti-microbial, Eliminated motion artifacts	Material oxidation
	ECG	Polymer/Ag NWs electrode	Highly stretchable, low sensing limit, and good durability	Requires tight contract
	ECG	Graphene, textile	Easy to make	High noise
	ECG	PEDOT: PSS, LIG	Prolonged stability, High waveform quality	Prone to motion artifact

	ECG/EMS	PDMS	Scalable, less skin irritation	Prone to motion artifact
	ECG	Ag/AgCl	Wi-Fi wireless transmission	High power consumption, short lifespan
	ECG	Ag/AgCl	Low power consumption, dry 3D printed electrodes	Short battery lifespan
	EMG	Ag, nylon plastic	Convenient, real time processed	Data accuracy
Non-contact sensor	ECG/EMG/EEG	PS25255 EPIC	Portability, long-term monitoring	Poor tight contact, prone to motion
	ECG/EMG/EEG	Flexible printed circuits (FPC)	Flexible, no obvious power frequency noise	Baseline drift exists
	ECG	ASOPA4002	Completely flexible and ultra-thin	High power consumption
	ECG	Silicone-based sensors	Comfortable, noise immunization	Short monitoring period
	ECG	Silicone dry electrode	Reliable, low power consumption, low cost	Irregular waveforms, low CR
	ECG	PDMS-Graphene	Textile based, high quality	Limited stability
	ECG	Graphene	Soft, low cost, scalable	Contact impedance exists

Implant-able	Peripheral neural signals	TiO2, silicone	Good biocompatibility	Unknown mechanical properties

Table 1 lists some typical examples of wearable vital signs monitoring, as well as relevant features and limitations for comparative analysis.

2.1.1 Wearable sensors

The applications of wearable sensors are widespread in many fields such as in the medical, education, and security (for example in motion detectors or doors), this is because they provide a good amount of accuracy, they are reliable, and they can provide real-time information that can assist individual users to detect possible problems. All the mentioned features are useful in the medical field that can be applied to monitor diseases, diagnosis, treatment, and healthcare management. These wearable sensors are intended to operate on the human body, therefore, both hardware and software should be designed according to standards, and safety requirements to avoid physical injury, which is medically and engineering not easy to achieve [10]. We also, need to be careful and differentiate between medical sensors and wearable sensors because not all wearable sensors are medically certify.

Nowadays, wearable device companies are offering various new products including fitness trackers, watches, smart-clothing, head mounted displays, and implantables.
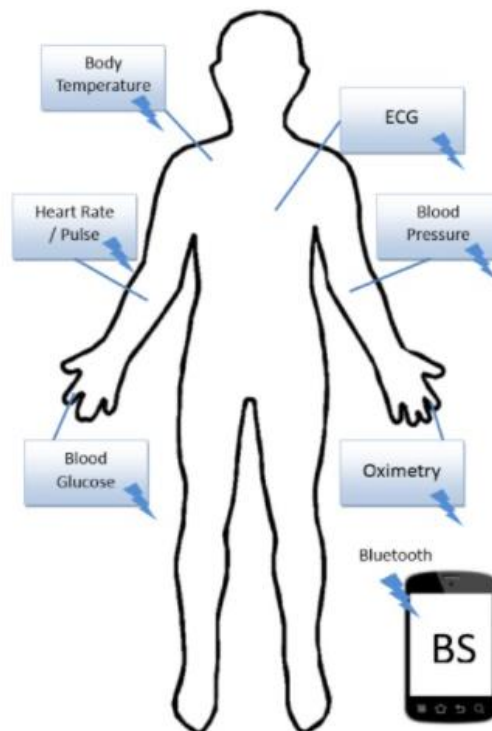
Figure 2. Wireless body sensor network [10].

Figure 2, has shown some wireless physiological sensors that can be used for data collection of a patient's vital signs. The sensors can be grouped into, intrusiveness (invasive) and non-intrusiveness (non-invasive). Non-intrusiveness sensors can measure a patient's physiological data without the devices inserted into the human body but rather, on the skin surface, an example of such is temperature sensors and an ECG. While the intrusiveness sensors detect physiological signs by inserting a device into the human body, a blood glucose sensor is an example [10].

Over the years, many wearable sensors and devices had been proposed by both researchers and industries [11]. Some of these wearable sensors are envisioned to combine Bluetooth with an ECG, temperature sensors, heart rate, movement detector, and other features which are attached to the body or integrated with clothes to acquire physiological data. With the help of wireless communications, the data is transmitted to a remote server for monitoring. It is good to note that many of these wearable sensors are not medically certified.

2.1.2 Safety of wearable sensors

For the smooth operations of wearable devices, both the hardware and software are at the forefront. This is because we need to consider the weight, size, low energy consumption, security, and other factors that will help reach the safety requirements and to avoid physical injury, which is of great concern. Over the years, researchers in wearable devices have described that the proper designing of sensor components, their energy consumptions, and optimization will reduce the physical effects of sensors operation on our bodies, especially when they are placed directly on the body [10]. Others have suggested that the threat of thermal injuries to our tissue can be reduce by restriction of the sensing frequency, computation power, radio duty cycle of the sensors, and the radio frequencies of wireless networks.

Every country has its applicable regulatory requirement for wearable devices. Medical devices are now subject to strict controls and regulations by authorities, all around the world. For example, in the EU, all medical devices need to obtain a CE mark from the regulators, if all reguratory requirements are satisfied, before the product is clear for marketing. To obtain this clearance, the manufacturer has to provide the necessary evidence, usually, the technical documentation that their device meets general safety and performance requirements set by the EU Medical Device Regulators, and the device has to be reviewed by the panel of experts. While in the US and Canada, the device is required to be cleared or licensed by both the FDA and Health Canada before placing on the market. The technical documentation will be provided to both regulators depending on the device classification [11].

All wearable technologies require a certain kind of testing and verification by the regulators before they can be certified for use. The following type of testing reports is used in regulatory technical file submissions electrical safety, battery safety, toxicology, electromagnetic compatibility (EMC), interoperability, usability, wireless testing, and others. The risk of human body exposure to electromagnetic fields is regulated by many countries and that is why EMC requirements for both medical, and wearable devices are standardized. The safety and performance of wearable devices that are used in conjunction with other devices are important and need to be considered [11].

All medical devices must adhere to the international standards IEC62304, IEC 60601, and ISO 13485, which are examined to specify regulatory limits during design, pre-clinical validation, and validation of devices using wearable sensors as critical components [12].

2.1.3 Wireless protocols

There are many types of wireless protocol networks, as described in figure 3. The use case of every system is usually determined be which type of network that applications would operate on. A common division of network types is illustrated in figure 3 below where a range and computational power are key parameters.
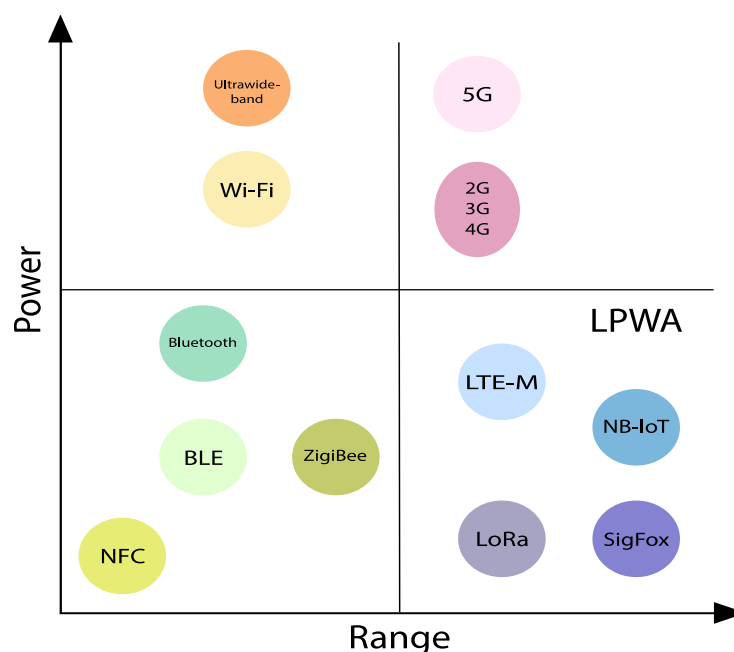
Figure 3. Wireless network types and Power Range.

In figure 3 above, we can see that the low-range and low-power applications include Near- field communication (NFC), Bluetooth, BLE and ZigBee. Lets keep in mind that the choice of wireless communication protocol needs to be made with an understanding of the major factors motivating a given product's wireless needs. It is useful that we compare a few characteristics of the wireless networks that will help us to understand, and to determine when to use which technology. As shown in figure 3, above Bluetooth, for example, offers the lowest power consumption and good range communications. Bluetooth low energy (BLE) is the focus of this thesis wireless communication protocal. Over the years, wireless technologies have made significant progress, and they are being integrated into many applications. Bluetooth in-particular has seen increased use in variety of applications most especially in medical field [13].

Medical devices just like commercial applications also face some development issues that can be addressed with wireless networks. The ability of Bluetooth to allowed mobile

27

connectivity is well suited for cable replacement. Bluetooth also provide other features such as security and reliability and can coexists with other wireless networks, and also it a low cost technology to implement [13].

The implementation of bluetooth in medical devices has helped in cable replacement. It has replaced the traditional RS-232 which ahs low data rate connections used in many medical devices. Bluetooth uses IEEE standardized technology (802.15.1) that allows connection with off-the-shelf components and enables connectivity for both to local-area networks (LANs) and wide-area networks (WANs) through access points and cellular mobile phones [13].

2.1.4 Power consumption issues

Wearable devices are becoming very popular and acceptable as people become aware of monitoring and improving their wellness, as discussed in section 2.1. And while there is continous improvement in current technology, there are still many problems that we need to overcome that will help enhance the overall user experience. For these devices to be commercial, they are designed to be portable and comfortable to the user while also offering advanced features and long battery duration. Unfortunately, all these design requirements often in conflict. The sizes of electronic components are becoming smaller, and with more features added, both improvements will assist the designers of wearabel devices. These additional features will increase the device complexity and computational power which can lead to a rise in the device's total power consumption.

Due to the necessity to recharge or replace the battery, battery life is one of the issues that limits how wearable devices may be utilized. With new functionalities added to the wearable devices, there is more strain placed on the battery power to operate. With the advancement in low power consumption technology and in wearable technology, and the number of connected devices in circulation has increased, and more wearable devices are estimated to be connected in the coming years [14]. While there are potentials for wearable devices and the positive impact they will have over users, the need to replace batteries every year and constantly charging them is a big obstacle that needs to be addressed.

Over the years, there have been improvements in mobile computing compare to batteries which has seen less progress in terms of technological elements such CPU speed, memory capacity, RAM, wireless transfer speed and others. To be able to

improve the battery capacity, it is also important to not only focus on the battery but also the components which are consuming the energy [14].

2.2 Vital Signs

Vital signs consist of blood pressure (BP), pulse rate (HR), respiratory rate (RR), temperature and where applicable blood oxygen saturation. The provide critical information about the patient's state of health [15]. The main function of the vital signs are they identify the existence of a sensitive medical condition, they can put out chronic diseases stages, example hypertension and they are a means of quantifying the magnitude of an illness and how the body is managing the illness.

2.2.1 Pulse rate (HR)

Pulse rate or heart rate (HR) is the number of times the heart beats in a minute. When the heart pumps blood arteries, these arteries will expand and contract with the flow of the blood. Taking the pulse measurement does not ony measure the heart rate, but it also indicate heart rhythm and strength of the pulse. The pulse rate of a healthy adult ranges from 60-100 beats per minute. These pulse rate might varies and fluctuate during exercise, injury, emotions, and illnes The HR is a vital sign and has become a standard measurement in both healthcare and sport activities. The monitoring of our HR will provide information its status by indicating changes in the heart cycle. The HR can be extracted from the ECG or PPG signals. Heart rate variability analysis is gaining attention as a simple indicator of the health status of the cardiovascular system [6].

2.2.2 Blood pressure (BP)

Blood pressure (BP) is the pressure against the walls of our arteries during the contraction and relaxation of our heart. The arteries carry blood from the heart to other parts of our body [16], [17]. Every time the heartbeats, blood is pump into our arteries, and it causes blood pressure to be at the highest, as the heart shrinks, and when the heart relaxes, the blood pressure falls. Throughout the day, our blood pressure varies, it rises and falls.

In blood pressure measurement, two values are recorded the higher value is called systolic pressure and the lower value is the diastolic pressure. Systolic pressure is the pressure inside the artery when our heart contracts and pumps blood through the body and diastolic pressure is the pressure inside the artery when our heart is at rest and it can indicate cellular oxygen delivery [16]. BP is recorded as millimeters of mercury. BP is influenced by some human physiological characteristics such as cardiac output, blood volume and viscosity, and vessel wall elasticity, peripheral vascular resistance [6], [17]. If one's blood pressure is high, this puts some extra burden on the heart blood vessels, and other organs such as the kidney, brain, and eyes. When the blood vessels are subjected to persistent high blood pressure, this will increase the risk factor of serious injuries and potentially life-threatening health conditions.

High blood pressure is also called hypertension, this is when the blood pressure is higher than the normal level. It is normal for our BP to change during the day based on the activities we perform. Having our BP consistently above the normal level may increase the chances of getting diagnosed with high blood pressure [17].

BP can be categorized as, normal, elevated, stage 1, stage 2, and hypertensive crisis high blood pressure described in table 2.

Tabel 2 Blood pressure stages [16], [17].

Blood Pressure Categories	Systolic mmHg (upper)		Diastolic mmHg (lower)
Normal	Less than 120	And	Less than 80
Elevated	120-129	And	Less than 80
High Blood Pressure (Hypertension) Stage 1	130-139	Or	80-89
High Blood Pressure (Hypertension) Stage 2	140 or higher	or	90 or higher

Hypertensive Crisis (Seek emergency care)	Higher than 180	Or	Higher than 120

Table 2 above shows the five stages of hypertension. The high stage of BP can directly increase the threat of heart failure, stroke, and heart attack. The arteries of a high BP patient will increase their resistivity against the flow of blood, and it will cause the heart to pump harder to help circulate the blood.

2.2.3 Cardio output

Cardiac Output (CO) it is the amount of blood our heart pumps through the circulatory system per minute. For our body to function normally, the heart needs to pump blood that will be sufficient and adequate for continuous supply of oxygen and nutrients to our vital organs and brain. Our body demand for oxygen changes. For example during exercise, the CO is altered by modulating both our heart rate and stroke volume. This is because our body may need three to four times the normal CO due to the need of more blood by our muscles. The heart beats faster and stronger to help increased the CO during exercise [18].

Cardiac Output is an interesting hemodynamic parameter. It can be mathematically stated as, CO is equal to heart rate and stroke volume and it is expressed in L/ min. CO is useful in the assessment of cardiovascular disease, for example patients with coronary artery disease or with congestive heart failure. Although, the accurate measurement of CO is based on invasive methods. Invasive methods might be dangerous and complicated, which can increased mortality in critically ill patients, and require qualified practitioner [19].

2.2.4 Hemodynamic parameters

Hemodynamics is referred to the movement of and the general principles that are governing the flow of blood in our human body [20]. Hemodynamic parameters include heart rate and blood pressure while the advanced parameters are stroke volume, cardiac output, and total peripheral resistance [21]. The measurement technique primarily CO, utilized an invasive pulmonary artery catheter and an arterial for seriously ill patients. The movement and flow of blood throughout our body are dependent upon other factors.

Pressure differences and resistances are two of the most important factors between the different elements of the circulatory system, such as the cardiac chambers, arterioles, venules, veins, and, large arteries. Along with HR, pressure and resistance are vital determinants of the amount of circulatory blood flow. The measurement of hemodynamic parameters, like blood BP and HR, can be determined non-invasively [20], [21].

2.2.5 Oxygen saturation (SPO_2)

Oxygen saturation (SpO$_2$) is the ratio of oxyhemoglobin (oxygen-bound hemoglobin) to the total concentration of hemoglobin. SpO$_2$ is a vital parameter that can be used to define the blood oxygen content and oxygen delivery in our circulatory system. The hemoglobin consists of four globular protein subunits at its molecular level and each subunit is linked a group of heme. Therefore, each molecule of hemoglobin has four heme-binding sites ready to bind with oxygen. The blood pressure, heart rate, body temperature, respiratory rate, and the SpO$_2$ are all vital parameter [22].

What happens when oxygen saturation drops in the body? When there is low-level oxygen in our blood that is lower than 90%, is known as hypoxemia and it can result from cardiopulmonary complications such as sleep apnea, certain medicines, and high-altitude exposure. The decreased in oxygen saturation is know as desaturation or and it can be caused by changes in several of variables.

The measurement of SpO$_2$ is important for patients with health conditions that may reduce the level of oxygen in their blood. Some of these conditions include heart failure, lung cancer, heart attack, chronic obstructive pulmonary disease, and other cardiopulmonary disorders. There are two methods to measure the blood oxygen level in our body, arterial blood gas, and pulse oximetry [22], [23].

An arterial blood gas is an invasive blood test that measures our blood oxygen and can detect the level of other in our blood as well as the pH.

Pulse oximetry has transformed modern medicine. This is because of its ability to monitor oxygenation in a continuous, accurate, and non-invasive way. As discussed in chapter 1, there is a need for low-cost physiological monitoring solutions that are easy to use, accurate, and can also be used, in the home or in ambulatory settings. Pulse oximetry can used to monitor continuously the arterial blood oxygen saturation of both adults and children. Pulse oximetry is not only limited to medical use. Pulse oximetry

ambulatory monitoring features a particular interest within the evaluation of aerobic efficiency of an individual undertaking a routine exercise [6].

2.3 Impedance

Impedance (Z) or admittance for its reciprocal value, it is the ratio between voltage and current. It applies to both alternating current (AC) and direct current (DC). While admittance is the inverse of impedance that is, not impede, but admit, current flow. Impedance is "the measure of a circuit's opposition to a current when a voltage is applied" . It has been introduced by the Oliver Heaviside in July 1886 followed shortly after with the admittance, which is   the inverse of the impedance. Immittance is the combined term for impedance and admittance [7]. Electrical impepedance is a measure of oppositionto a sinusoidal electric current. According to the definition, impedance can be described also as current response to the voltage excitation, or vice versa. The impedance is characterizing the object under the study and depends largely on the size and composition of the object.

One may ask why do we need to measure impedance, this is because impedance is an AC property it cannot be easily measured like resistance. For example, connecting an Ohm meter across the input or output of an amplifier „might" indicates the DC resistance or probably not even that. It is quite possible however to measure input and output impedance at any frequency using a signal generator, an oscilloscope (or AC voltmeter) and a decade resistance box or a variable resistor [7].
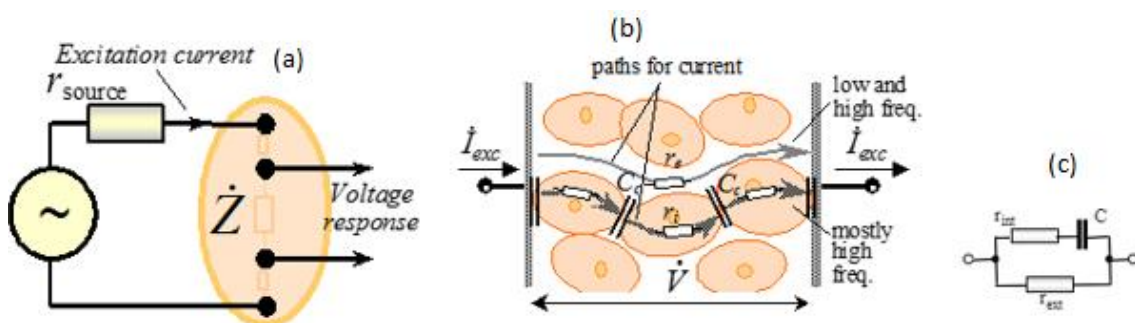
Figure 4. Electrical equivalent circuit of biological cells [24].

Figure 4 represents the electrical equivalent circuit of biological cells. In figure 4a, it describe the definetion of impedance, how current response to the voltage excitations

and figure 4c, represents the three element RC circuit, commonly used to discuss impedance of the tissue, also known as Cole type A circuit.

It is no longer sufficient to do a single measurement at a single frequency to characterize a circuit. A semicircular line is drawn on the phasor diagram for the frequency dependent impedance vector of the series connection of resistor and capacitor with parallel resistor, figure 5 [25].
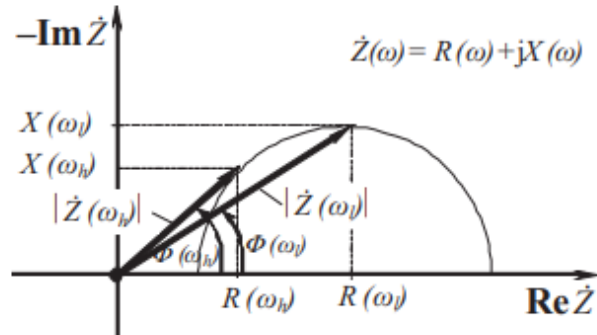
Figure 5. Graphic derivation diagram of the phase angle and its relation to resistance (R), reactance (Xc), impedance (Z) and frequency of the current applied [25].

Figure 5, represents a frequency response of the three element RC electrical equivalent circuit in figure 4, it can be expressed with acceptability through the impedances low and high that are measured at two frequencies the low and high. It is important to stress out that the impedance variations at a decade or more of distant low and high frequencies are also essentially different [25].

Impedance (Z) is the obstruction to the flow of an alternating current and it is dependent on the frequency of the applied current, defined in impedance magnitude (|Z|) and phase angle (φ), as shown in equation 1-3 [26].

$$\dot{Z} = \frac{\mathring{U}}{\dot{I}} \tag{1}$$

$$Z = R + jX_c \tag{2}$$

$$|Z| = \sqrt{R^2 + X_c{}^2} \tag{3}$$

$$\Phi = tan^{-1}\left(\frac{X_C}{R}\right) \qquad\qquad (4)$$

Resistance of an object is determined by a shape, that is described as length (L) and surface area (A), and material type, that is described by resistivity (ρ), as shown in equation (4) [26].

$$R_{(ohm)} = \rho(\Omega.m)\ \frac{L_{(M)}}{A_{(M^2)}} \qquad\qquad (5)$$

2.3.1 Impedance cardiography

Impedance cardiography (ICG) incorporate methods that provide analysis of trans-thoracic electrical impedance and its time dependence on blood volume, circulation, and cardiac function [27]. The analysis of ICG signals are used to diagnosis patients with cardiovascular diseases . ICG is a noninvasive approach to the measurement of the cardiodynamic. The ICG is modulated by cardiorespiratory activity, such that when there is a decrease in impedance, this can be related to an increase of blood flow. The derivative of impedance (dZ/dt) contains a set of points that is shown in figure 8. Cardiovascular condition and various hemodynamic parameters like the heart rate, stroke volume, vascular resistance, cardiac volume, cardiac output, and others, can be noninvasively monitored against time by extracting characteristic points and periods of the dZ/dt signal through ICG [27].

2.3.2 Impedance cardiography measurements

Impedance cardiography is a non-invasive tool of monitoring electrical impedance changes in the thorax. Research on ICG dated back to the 1940s and the technology development was in the 1960s [27]. ICG is considered a diagnostic technique for measurement of electrical impedance properties of biological tissues in the thorax. The principle of ICG technique is by applying a constant, alternating, high frequency and small amount of current through two outer electrodes placed on the skin and then acquiring the electrical voltage difference by using two inner electrodes. Tetrapolar-band electrode configuration setting has been used to record the thoracic impedance changes during the cardiac cycle [19]. The electrodes are placed around the abdomen and the upper part of the neck, while the sensing electrodes are fixed around the thorax and the lower part of the neck. An example is demostrated in figure 6.
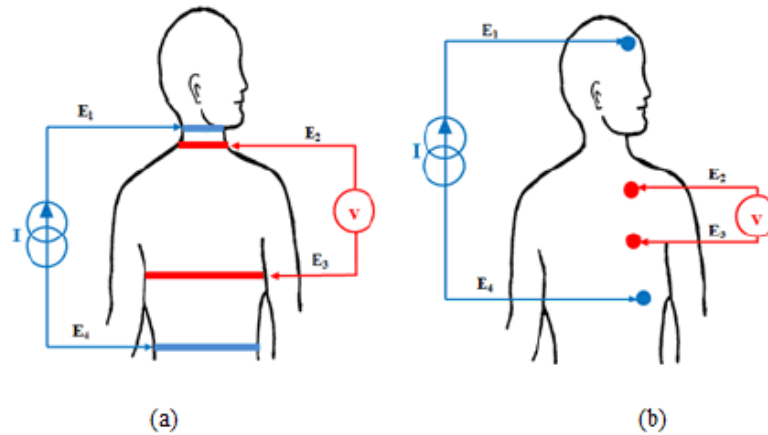
Figure 6. Electrode configurations for the impedance cardiography ICG signal measurements (a) tetrapolar-bansd electrodes, (b) tetrapolar-spot electrodes [19].

In figure 6 above, the tetrapolar-band electrode setting is shown in figure 4a, where E1 and E4 are the outer-band electrodes, E2 and E3 are the inner-band electrodes which are placed around the base of the neck. The four-band electrodes have been replaced by four-spot electrodes in order to ameliorate and facilitate measurements. Another electrode configuration has been described, as shown in figure 4b. It consists in injecting a current of 1 mA at 30 KHz through two outer electrodes (electrodes E1 and E4) that are placed into the forehead and above the leading edge of the heart; the electrical voltage difference is measured by two inner electrodes (electrodes E2 and E3) which are placed between the outer electrodes, precisely on the left side of the patients' chest [19].

2.3.2.1   Impedance cardiography recording

Ohm's law defined impedance (Z), as the ratio that ia between the measured voltage and the injected current signal [19]. This measure voltage is proportional to the impedance variation. Therefore, when the current strength is known, impedance can be calculated. ICG recording is denoted by dZ/dt, which is the first derivative of the impedance variation signal (ΔZ) [19]. Figures 7 and 8 are examples of ICG recording from a patient that can later be anlyzes.
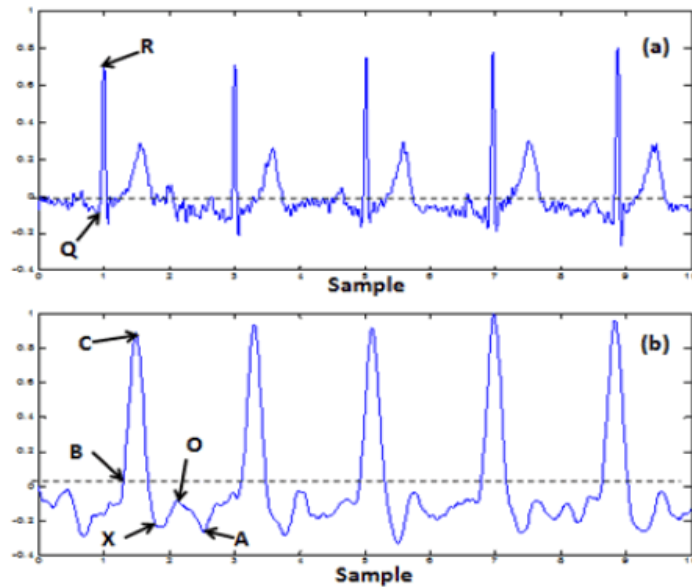
Figure 7. ECG tracing, (b) characteristic point in impedance cardiography ICG tracing [19].

Figure 7, shows an example ICG recording and its main characteristic points, that are distinct physiological events in the cardiac cycle. Point A presents the start of electromechanical systole, and it is related to the volume change happening because of the dynamic atrial withdrawal. Point B is used for calculating the stroke volume and cardio output, it denotes the beginning of the ejection time, and it appears simultaneously with the opening of the aortic valve. There are various methods to identify the location of point B, and the precise identification of this point is important to ensure the accuracy of stroke volume and cardiac output. Point C is taken at the peak of the ICG trace, and it corresponds to the ventricular contraction, while point X is the lowest point after peak C, it is synchronized with the conclusion of the aortic valve, and it demonstrates the finish of the systole stage. Finally, point O is associated with the changing of the volume during the diastolic phase of the cycle and the maximal opening of the mitral valve [19].
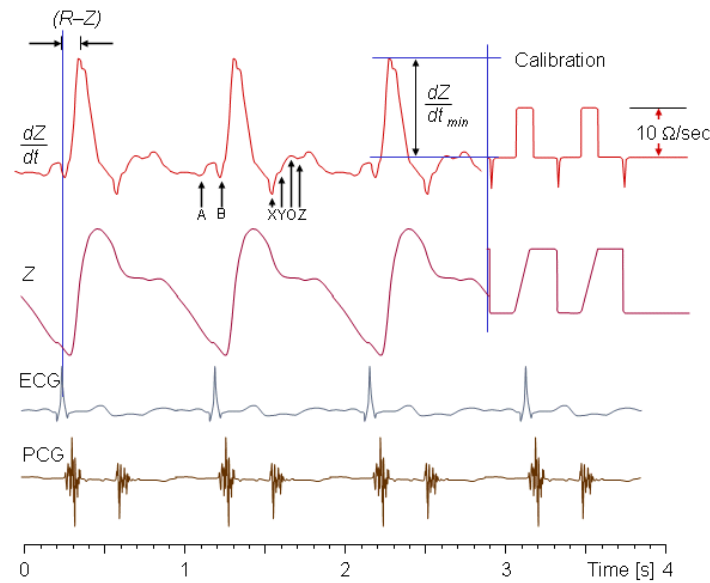
Figure 8. Thorax impedance curve [28].

Figure 8 presents a typical thorax impedance curve (Z), its first time derivative (dZ/dt), and the simultaneous electrocardiogram (ECG), and phonocardiogram (PCG) curves. The impedance curve is usually shown so that a decrease in impedance results in an increase in the y-axis magnitude. This sign convention describes the changing admittance; for example a decreasing impedance could arise from an increasing amount of low impedance blood in the thorax. The polarity of the first derivative curve is consistent with the impedance curve [28].

2.4 Acquisition of Electrical Bioimpedance

Bioimpedance is the measurement of the opposition that a biological matter presents to a current when a voltage is applied. Both bioimpedance and bioelectricity are in reference to biomaterials in general. „biomaterials can be alive, have lived, or serve as a host to living tissue". This tissue may be from a plant, fruit, fish, animal, or human body. A living cell is a building block, and a precondition for its life is that it is encircled by an electrolyte solution [7]. Bioimpedance is concerning the electrical characteristics of our body or other biomaterials. For example to what extent is our body good electrical conductor? Bioimpedance is a measure of how good our body impedes electric current flow [7], [29].

Bioelectrical impedance helps in providing information about the tissue structures and its states. The bioimpedance measurements in humans have received a considerable

attentions during the past years, because it has many advantages, such as „low cost", easy application, it is noninvasive and it has good monitoring capabilities [29]. The analysis of bioimpedance helps in the detection of physiological changes in cell to cell, cell matrix interactions caused by the effect of viral and bacterial infections, toxicity, environmental parameters, and the effect of pharmaceutical compounds. Also, electrical investigation of biological materials has been performed over the past century, using both conventional electrodes and microelectrodes [30].

Bioimpedance method work injection into a biological object, for example human body, tissue or cell of an alternating electric current of very low intensity. The voltage drop caused by the electric current is proportional to the electrical impedance of the tissue, the higher the voltage drop, the greater the electrical impedance of the tissue. Bioimpedance measurements are based on the notion that, depending on their changes, biological mediums behave as conductors, dielectrics, or insulators of electrical current. As a result of this phenomena, bioimpedance readings are dependent on frequency, which can provide information on tissue and cell function and pathology [27].

2.4.1 Tissues

The first experiment carried out regarding the electrical properties of tissue have been proposed by Hber from 1910 to 1913 [31]. He has described that the cell membrane is an electrical isolator, while extracellular and intracellular fluids are resistive in nature. From this observations the author Cole. S.K deduced the electrical equivalent circuit shown in figure 9, also known as the Cole-Cole-Model [31]. For low frequencies, the current cannot pass the isolating membrane and flows completely around the cell resistor. For higher frequencies, the current passes the capacitive membrane and a part of it will flow through the intracellular space resistor. Current paths for both cases are shown on the left side of figure 9 [32].
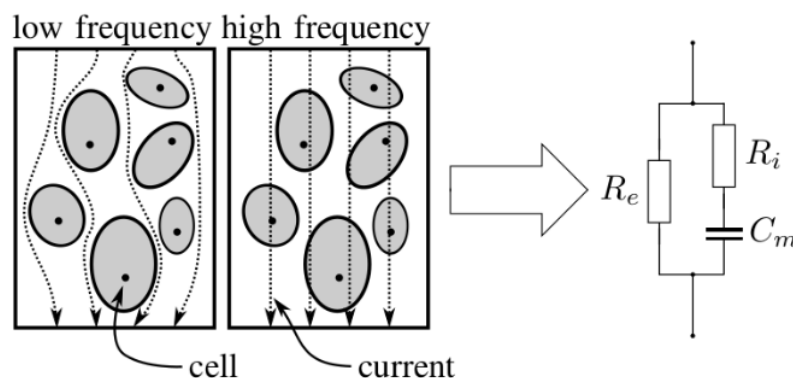
Figure 9. Equivalent electrical circuit of tissu [32].

39

The electrical impedance of biological tissues is known as bioelectrical impedance. The electrical impedance of the biological tissue depends on the electrical properties of the biological tissues and the property of the electrical signal applied. Biological tissues are conductors and their resistance varies with frequency. The electrical property of any biological tissue depends on its inherent structure.

Impedance is measured by applying a small electric current, for example on two electrodes and getting the resulting voltage with another pair of electrodes. The lower the voltage the lower the tissue impedance for a given current. Figure 10 shows an example with electrodes around a cylinder, for instance skin surface band electrodes around an arm or a leg [29].
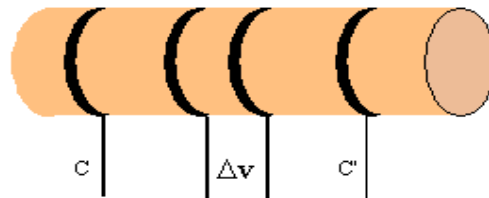
Figure 10. Bioimpedance and Bioelectricity Basics [30].

Tissue is made up of cells and membranes, which are thin but have a high resistance and act as little capacitors electrically. The current goes right through these capacitors when high measuring frequencies are used, and the result is dependent on tissue and liquids both inside and outside the cells. The membranes, on the other hand, obstruct current passage at low frequencies and the results are solely reliant on liquids outside the cells [29].
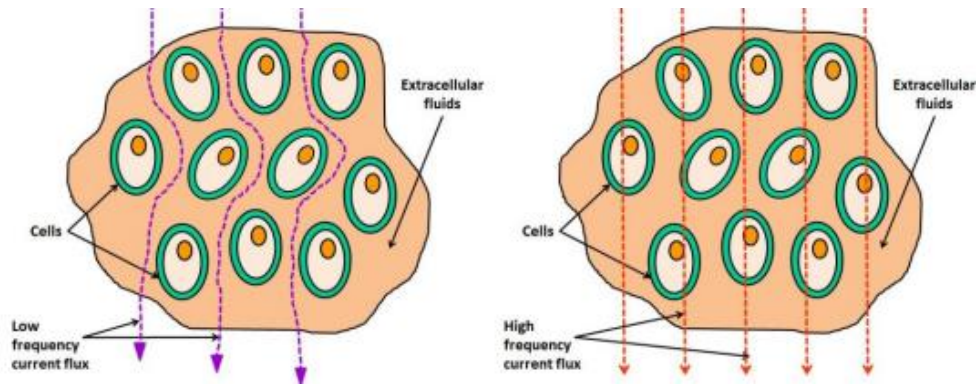
Figure 11. Electrical current conduction through biological tissues (a) current conduction through biological tissue for low frequency signal, (b) current conduction through biological tissue for high frequency signal [32].

In figure 11 illustrates, a low amplitude electrical signal is injected into two different frequencies. Figure 15a is a two electrode method of current injection while figure 15b is a four electrode method [32].

2.4.2 Disturbing factors

The use of bioelectrical impedance is widespread both in healthy people and patients. EBI monitoring is a arising technique for medical and biomedical research practice. It establishes one of the symptomatic strategies dependent on the investigation of the uninvolved electrical properties of the natural tissues. Biological tissue properties have been a subject of research when Luigi Galvani (1737-1789) [33] discovered that while his assistant was touching the sciatic nerve of a frog with a metal scalpel, when he drew an electric arcs on a nearby electrostatic machine, the frog's muscle moved. Furthermore, these properties started to be measured by the end of 19th century, when James Clerk Maxwell (1831-1879) developed a new instrumentation and the setup of the electromagnetic field theory [33]. The practical application of electrical passive properties kick off in the mid of the 20th century. Various properties and procedures resulted in a set of ways that are presently employed for multiple applications [33].

The contribution of electrode polarization impedance to the test result is theoretically excluded in tetrapolar bioimpedance experiments [34]. When a current is injected into a tissue or volume conductor by two electrodes, the potential difference between them is measured by a different electrode pair. Therefore, the unknown impedance can be calculated by dividing the voltage drop by the injected current. The result will be incorrect if part of the injected current takes a different part other than that between the potential electrodes. When measuring large volume conductors at higher

frequencies, stray capacitance from the body to ground provides such a possible distinct path. Tetrapolar bioimpedance measurements can be implemented by two methods. The first method is to apply aknown curent and the drop involtage is measure, while the second method is to apply a voltage and measure both the resulting current and the drop in voltage [34].
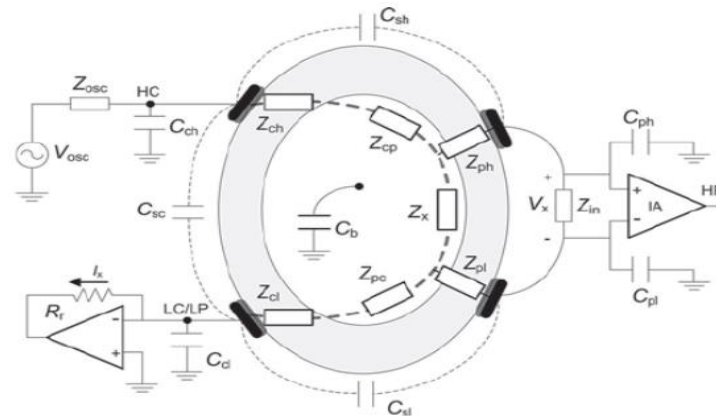
Figure 12. Stray capacitances in impedance measurements performed with four electrodes [34].

The circuit in figure 12 is a models tetrapolar bioimpedance for performing measurements. The impedances of current electrodes have been divided into two parts, electrode skin interface and body impedance between each current electrode and the closest potential electrode. These two potential electrodes are connected to an instrumentation amplifier which has input impedance that will affect the measurement. Hence, if the current injected into the body and the voltage drop between the potential electrodes is measured, then the result will be change by the presence of the components such   Csh , Csl, Csc and others as shown in figure 12 [34].
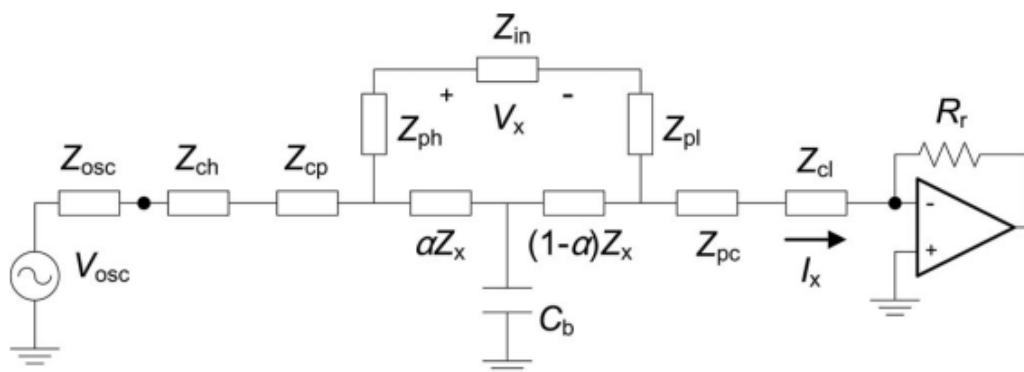
Figure 13. body to ground is much larger than the other stray capacitances between electrodes and from electrodes to ground [34].

The circuit model in figure 13, includes the impedance of each potential electrode the input impedance of the voltage amplifier, and the two segmental body impedances between each current electrode and the closest potential electrode [34]. The equivalent circuit used as an electrical model for the measurement of tetrapolar bioimpedance which includes the equivalent discrete circuit component for each of the electrodes and the voltage amplifier's input impedance, which is used to measure the actual voltage drop across the sample [34].

2.4.3 Electrode placement considerations

During the last decades the applications of measurements of electrical bioimpedance (EBI) to assess tissue contents or tissue status have increased, because there are several applications of EBI. EBI measurement is a noninvasive detection method comparable to microfluidic cell detection, however it concentrates on tissue rather than individual cells. The method is commonly used for medical purposes and it and works in conjunction with physicochemical and biological approaches. EBI applications include in ECG, impedance cardiography (ICG), electrical impedance tomography (EIT), and electrical impedance myography (EIM). Using the mention applications to acheive EBI measurement, a weak AC voltage or current signal is supplied to the body tissue, which consists of resistive body water and capacitive cell membrane. To assess the tissue's complex electrical impedance, a phase-sensitive technique is used to detect the resulting current or voltage signal [35].

Main problem in the EBI measurement is that small changes are often lost in large basal quantities. It may pose a serious challenge for the examiner, if those changes are of interest, and they often are. It requires wide dynamic diapason from the measurement apparatus in case of the direct measurement. Secondly abrupt changes in contact impedance, motion caused artifacts etc. may saturate the measurement channel for long periods, and cause slow wandering afterwards [36].
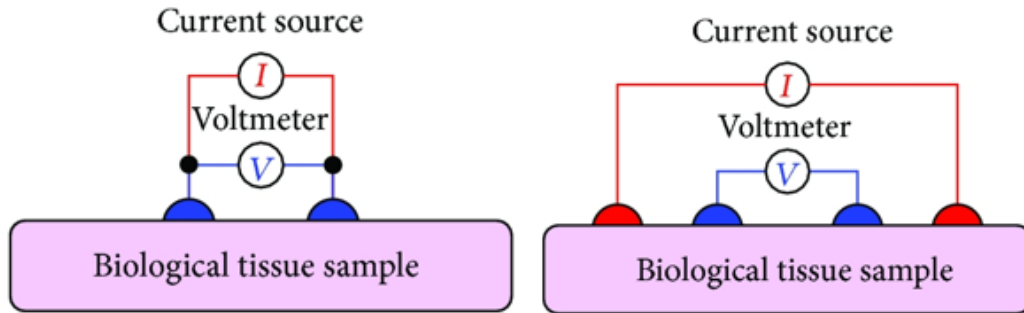
Figure 14. Schematic of impedance measurement with two-electrode and four-electrode methods (a) two-electrode method, (b) four-electrode method [37].

There two methods to conduct bioimpedance measurement process, electrode, or four electrode methods. The surface of electrodes through which the current signal is injected is called current electrodes shown in figure 14, (red colored electrodes) and the voltage electrodes are the electrodes that measure the frequency-dependent ac potential (blue colored electrodes)[37].

The two electrodes method shown in figure 14a, uses two electrodes for impedance measurement, both the current signal injection and voltage measurement are conducted with the same electrodes. The problem with this method, is that there is contact impedance, and as such the measurement data contains the voltage drop due to the contact impedance. While in the four electrodes method shown in figure 14. There are two separate electrode pairs that are used for current injection, and the voltage measurements. Therefore, the four electrode method is establish as an impedance measurement method which has a linear array of four electrodes that is attached to the system under test in figure 14b [37].

2.4.4 Wrist-wearable electrical bioimpedance

The development of wearable medical devices for continuous and noninvasive assessments of physiological vital signs and biochemical variables is having an impact on the healthcare system. This is because patients are turing from the conventional hospital centered system to an individual centered system [38]. The wrist is an optimal measurement site for the patient's comfort and it's a practical place to wear a monitoring device. Physiological signs on the wrist, on the other hand, have small amplitudes, requiring transducers that are capable with low signal-to-noise ratio and consequently having high sensitivity. Furthermore, during movement, the high sensitivity will be a set back because it will start to pick both motion movement and physiological data. Indeed,

wrist motion artefacts are very common in ambulatory situations. Acceptability, precision, and motion artefact resilience should all be considered when choosing a measurement method [39].

The measurement principle on the wrist is shown in figure 16 and 17. When an alternative current source is used to inject current in measurement site through the outter electrodes. Inner electrodes are then used to measure a resulting voltage signal proportional to the instantaneous impedance of tissues.
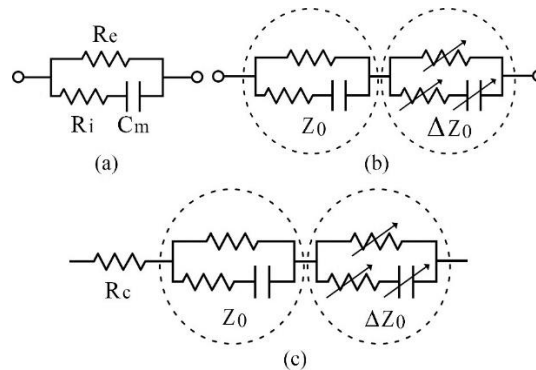
Figure 15. (a) Cole model of bio-impedance. (b) Impedance model of wrist tissue part. (c) Impedance model of wrist tissue part with the contact resistance [38].

Figure 15 show the equivalent electrical circuit of a tissue in the Cole-Cole model, shown in figure 15a, wrist biological tissue with an electrical blood model of heart related impedance variation can be modeled as shown in figure 15b. The basic tissue impedance and the impedance variation are most likely two aspects of the bioimpedance model of the wrist body part. Also, the basic impedance also contains the skin contact resistance expressed in figure 15c, in practical measurement. The primary goal is to get the low amplitude of the impedance variation from the static impedance. The measuring range for impedance variation can be expanded when the static impedance is corrected using a balancing system [38].

Electrode placement is crucial for accurately measuring disease progression and effectiveness of treatment. Figure 16 shows an example of 4 electrode placement on the wrist. The compound muscle action potential, for example, is known to be sensitive to modest changes in electrode position, whether the active electrode is put over the muscle's midway or the reference electrode is put over the joint or tendon. The shape and amplitude of the waveform recorded will change depending on the locations of the active and reference electrodes, and this effect will vary based on the muscle [40].
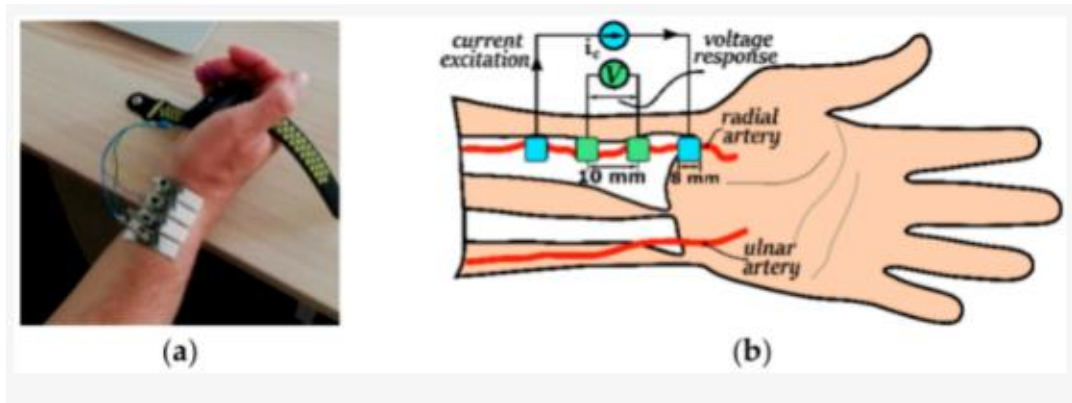
Figure 16. Electrodes (b) and their placement (a) during acquisition of the EBI [40].
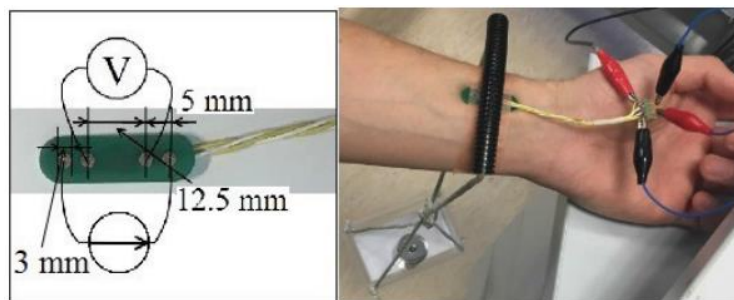
Figure 17. Electrodes used during data acquisition on the wrist [36].

Designing a wearable device for data aquisition has many challenging factors to overcome, and also few conclusion could be drawn from it [36]. Figure 17, depicted an electrodes used for bioimpedance measurement on the wrist. It is a FR4 printed circuit board with a gold plated electrodes used for data aquisition gathering. Placement of the phase angle base impedance is around -4 degrees. The phase angle modulation signal caused by blood pulsation is slightly higher ca -16 degrees, and the magnitude is roughly 200 times smaller than the, much less informative, value of the base impedance [36].

2.5 Electrocardiography (ECG)

Electrocardiogram (ECG) has become one of the most commonly employed non-invasive diagnostic tools that are used for recording physiological activities of the heart over a long time [41]. The data recorded from an ECG has helped in the diagnosis of many cardiovascular abnormalities, such as congestive heart failure, premature contractions of the atria or ventricles, atrial fibrillation, myocardial infarction, and other problems. There has been a rapid development of portable ECG monitor systems over the years in the medical field, such as the Holter monitor [42], [43], and other wearable devices in

various healthcare areas, like the Apple Watch, Samsung watch, and others. With this advancement in wearable devices, the amount of ECG data that requires analysis has increased human cardiologists to keep up. Furthermore, the idea of analyzing ECG data automatically and accurately has become a research topic over the years [41].

The ECG is a device that is used for measuring the electrical activity of our heart and provides an assessment of heart rate, rhythm, conduction, and repolarization from multiple lead vectors [3]. Holter monitors [42], [43] is an example of a portable ECG device that is used on patients to get data that can later be analyzed. The ECG, electrodes when they are placed on the body, they sense some tiny electrical charges of a heartbeat arising from the skin. When these electrodes are placed on a different part of our body, it gives a „comprehensive picture" of our heart's activities. For example, a 12 lead ECG device consisting of 10 electrodes when placed on the body. It can provide 12 different perspectives of the heart's activity using various angles among electrical planes. An example of a typical ECG of a healthy person is shown in figure 16, which provides information on whether heart activity is too slow, fast, irregular, or if heart muscles are being overworked [3].
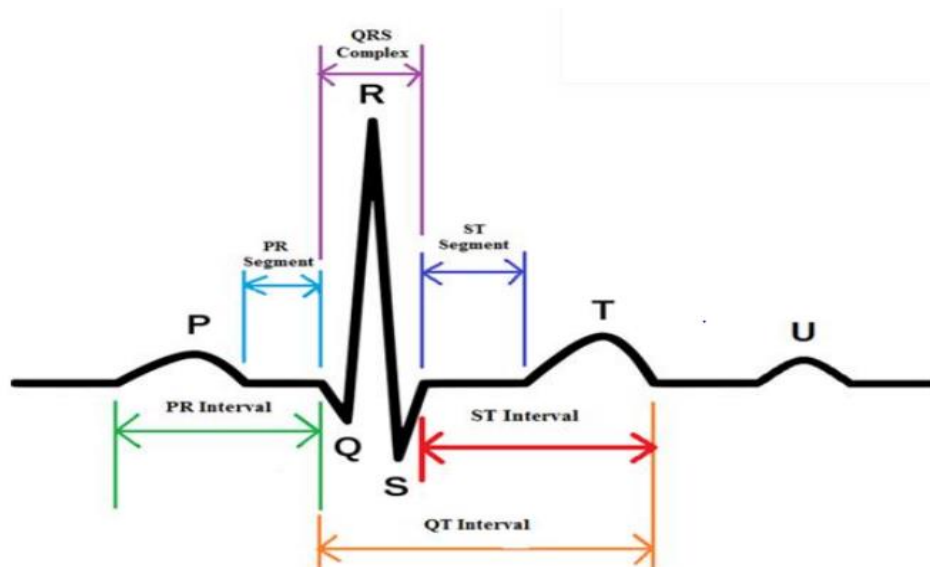
Figure 18. Schematic of healthy ECG waveform [3].

Figure 18 illustrate the ECG waveform lead. The ECG waveform is donated by five peaks and valleys, P, Q, R, S, T and U. Each of the waveform represents a change in electrical potential of our heart resulting in muscle activity and resultant of our heart movement. The R-peak is the different peak from the ECG result that is included in the QRS complex and it represents the ventricles depolarization where there is higher differential potential. The resultant of the R-peak is used to measure the heart cycles [6]. The heart

rate is derived from an ECG and it can provide information about the activities of the heart. For an adult the normal heart rate beating, ranges from 60 - 100 beats per minute. When the heart is beating too fast is known as tachycardia or when its too slow is known as bradycardia are types of cardiac arrhythmia. Integrating sensors into medical wearable devices can help in early detecting of cardiac abnormalities on patients [3].

The most basic ECG examination is with three skin surface electrodes on the limbs, one at the left arm (LA), one at the right arm (RA), and one at the left leg (LL). Figure 19 illustrates how six limb leads are derived from these three electrodes [7].
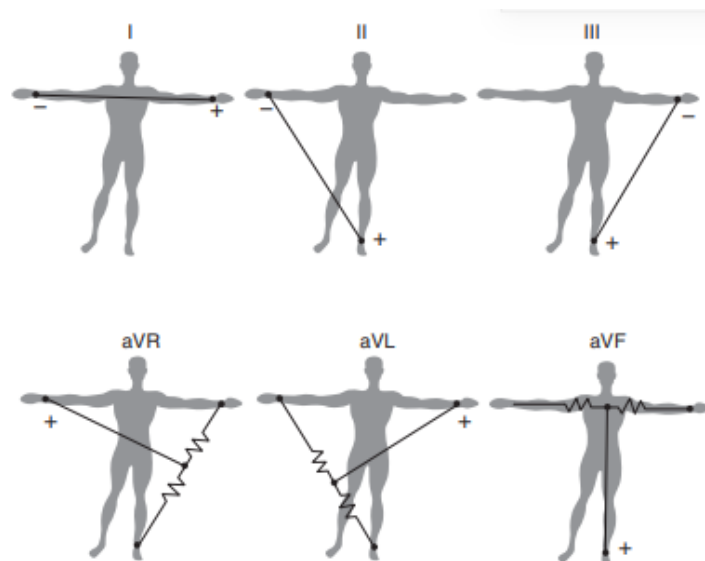
Figure 19. The six limb leads derived from three limb electrodes (both arms and left leg). Here, a indicates augmented [7].

Because the distal part of each limb is isoelectric (with regard to ECG, not, for example, electromyography (EMG) sources of the arm muscles), the location of the electrodes on each limb is not critical. The bipolar leads have such high repeatability that they are used to determine the axis of the electric cardiac vector. The ECG test is used to determine the electrical properties of the heart by measuring potential changes on the skin's surface. Currents in the surrounding tissue are produced by the heart's emfs. How the current flow spreads and which potential differences are discovered at the skin surface is determined by the morphology of the thorax and the conductivity distribution. The thorax tissue is thought to be linear with the heart's normal endogenous current density and electrical field amplitudes [7].

2.5.1 ECG technology

Electrocardiogram technology works by placing on our skin some small metal disks known as electrodes, and these electrodes can pick the electrical impulses that is produced by our heart. The electrical impulses are recorded together with the pattern that shows our heart's electrical activities. The electrical impulses from the heart originate from the electrical signal sent to the heart from the SA node. ECG technology in wearable technology is seen almost exclusively thin chest straps and harnesses. The strap or harness is used because the electrodes need to be nearest to the heart to pick up the electrical impulses given off by the heart. There are still barriers with ECG wearable technology. These barriers are mostly related to the user's anatomy, heart location, size, and body fat have the potential to effect heart rate readings. Also, electrode location in relation to the anatomical location of the heart could also produce inaccurate heart rate readings. The ECG technology relies on electrical impulses of the heart instead of blood profusion to the extremities and has fewer obstacles to overcome compared to PPG technology [44].

2.6 Photoplethysmogram (PPG)

There are other wearable devices that can be used for clinical physiological monitoring of our body. Photoplethysmogram (PPG) is an example. The PPG device is one of the widely used techniques for detecting of volumetric changes in our blood peripheral circulation. The PPG is „said to be a low cost" and non-invasive method that takes measurements on the surface of our skin [8]. The technique can provide information that is related to the cardiovascular system of our body. The device has two main components which include photodetector and the infrared light emitting source as shown in figure 20 below [8].
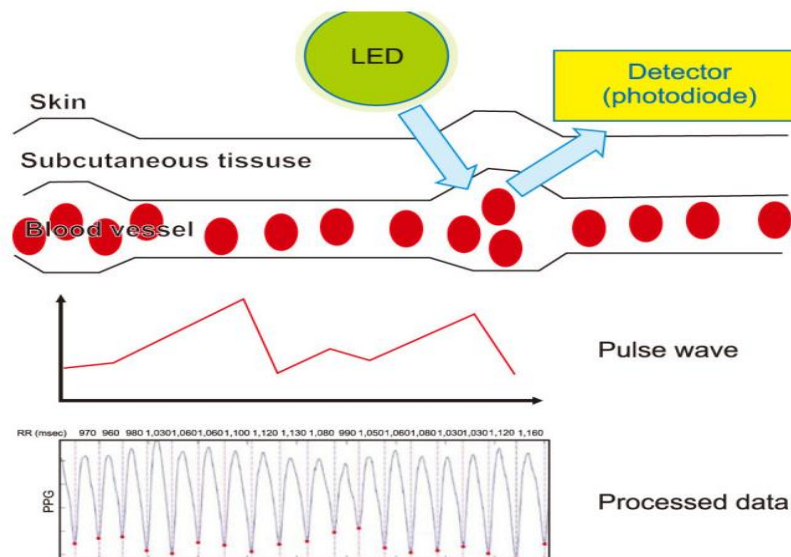
Figure 20. Brief diagram of Photoplethymogram (PPG) based heart rhythm monitoring [8].

PPG technology can be used in various medical applications such as in blood oxygen saturation, blood pressure, cardiac output, heart rate and others. As we discussed in section 2.4, the heart rate beat can be extracted from the peak detection value during electrical pulsatile nature of our blood vessels, and it could be matched with QRS wave of ECG. The application of PPG methods in wearable devices might have some potential because of its size and it has low electrical energy consumption. It can be modified into different shapes of devices such as wristwatch, smartphone camera, or fingertip detector [8]. PPG technology has gain some popularity as an alternative heart rate monitoring technique in recent years, this is due to the simplicity of how it is operated, the wearing comfort for its users, and its cost effectiveness. Although, one of the obstacles in using PPG techniques is its inaccuracy in tracking the PPG signals and light physical exercises. Some of the drawbacks is that the PPG signals are susceptible to motion artifacts caused by hand movement, and other alternative factors such as environmental noise may also affect the PPG signal acquisition that will result to inaccuracy estimation of the heart rate. Furthermore, PPG devices generate large amount of data making it difficult to interpret. However, recent acheivements in artificial intelligence field can provide a solution to overcoming this hurdle to better interpret data [8].

3 Selection of Tools

This section describes the hardware (tools) and software needed for the completion of this thesis as explained in chapters 1. It describes the reasons for the chip selection, why the electronics components and the embedded software are chosen. The microcontroller selected in this thesis is an analog device ADuCM350, based on a low power ARM Cortex-M3 processor. The bluetooth selected is a nordic semiconductor nRF8001 bluetooth chip. Additional components present are external 14bit dual channel ADC (ADS7946), ICM-20948, an external flash memory and SPO2 sensor MAX30101EFD+. The ADUCM350 software development kit (SDK) is made for IAR embedded workshops for ARM (EWARM).

3.1 AduCM350

The ADuCM350 microcontroller is a coin cell powered, high precision, meter-on-chip for portable device applications. This microcontroller is developed for applications such as point-of-care diagnostics and body-worn devices for monitoring vital signs. The ADuCM350 microcontroller is designed and configured as an impedance converter and potentiostat with current and voltage measurement capabilities which can be electrochemical sensors and biosensors [46] [47] [48].

ADuCM350 is an ultralow power, which is an integrated mixed-signal metering solution that includes a microcontroller subsystem for processing, control, and connectivity. The microcontroller subsystem is based on an ARM Cortex-M3 processor, an analog front end (AFE), a collection of digital peripherals, embedded static random-access memory (SRAM) and a flash memory and also, an analog subsystem that provides clocking, reset and power management capabilities [45][48]. Other features include the following in figure 21 below.

AduCM350 supports low dynamic and standby power management mode systems. The ADuCM350 provides a collection of power modes and other features like dynamic and software controlled clock and power gating. Power management unit provides the system with four different power modes that enable various levels of clock and power gating in order to minimize power consumption. When the system is in hibernating mode, the activity on peripheral interfaces or events ranging from the wake-up timer can wake up the device. The software controlled together with automatic clock gating are use to reduce dynamic power consumption, also power gating is also used to reduce standby current[48].

The analog front end (AFE) is connected to the ARM Cortex-M3 across an advanced high performance bus (AHB) slave interface which is on the advanced microcontroller bus architecture (AMBA) matrix, together with direct memory access (DMA) and interrupt connections [48].

- 16 MHz ARM Cortex-M3 processor
- 384 kB of embedded flash memory
- 32 kB system SRAM
- 16 kB EEPROM
- Integrated full speed USB 2.0 controller and PHY
- Power management unit (PMU)
- Multilayer advanced microcontroller bus architecture (AMBA) bus matrix
- Central direct memory access (DMA) controller
- I²S and beeper interfaces
- LCD controller functions
- Serial peripheral interface (SPI), I²C, and UART peripheral interfaces
- A real-time clock (RTC)
- An analog front-end (AFE) controller
- General-purpose, wake-up, and watchdog timers
- Programmable general-purpose inputs/outputs (GPIOs)
- A power-on reset (POR) feature and power supply monitor (PSM)
- A discrete Fourier transform (DFT) engine
- Receive filters
- Six-button CapTouch® interface
- 12-bit digital-to-analog converter (DAC)
- Temperature sensor
- Instrumentation amplifier control loop
- 16-bit analog-to-digital converter (ADC) performance
- High precision voltage reference

Figure 21. AduCM350 features[48].
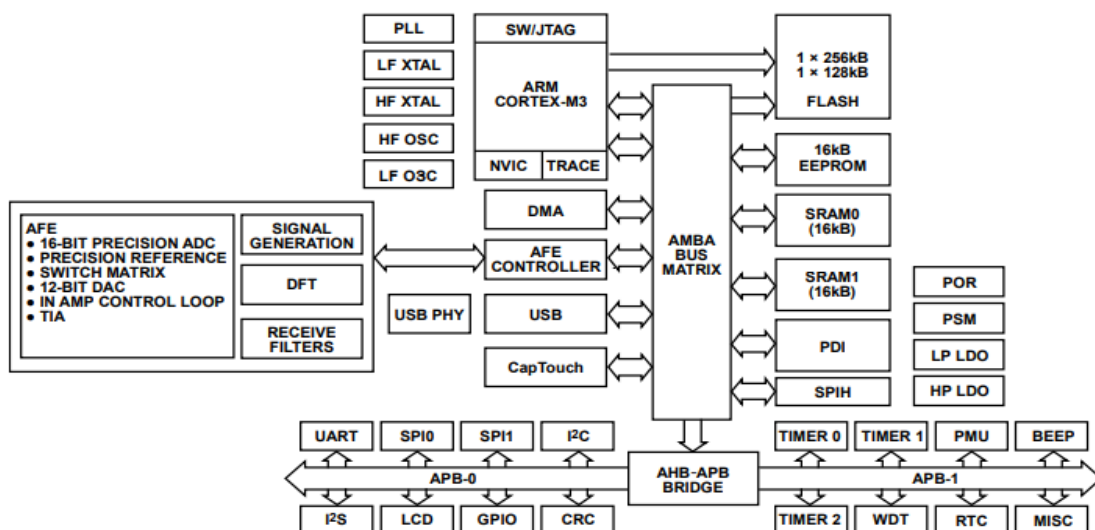
Figure 22. Functional Block Diagram of AduCM350 [48] .

Figure 23 above shown the system block diagram of AduCM350 with some of its features listed in figure 22. The AduCM350 is embedded with ARM Cortex-M3 which is a 32-bit reduced instruction set computer (RISC) processor, providing peak performance up to 20 MIPS at 16 MHz. A central DMA controller is used for moving data efficiently between memory and peripherals. It has on-chip nonvolatile flash of 384 kB memory, 16 kB of EEPROM and 32 kB of SRAM. ADuCM350 also, provides a range of flexible clocking features, this allows the system to operate from an internal RC oscillator, a crystal oscillator and a phase-locked loop (PLL). The device offers a range of programmable clock divisions, it allows software to run at the minimum clock frequency required to save power[48].

The system also integrates a range of on-chip peripherals. These peripherals can be configured via the microcontroller software for a given application. Example of these peripherals include UART, I2C, USB, I2S and SPI communication controllers, GPIO port, general timers, system watchdog timer and wake-up timer. The AFE features a 12-bit DAC, an ADC with 16-bit precision, an amplifier control loop, an integrated temperature sensor, a precision reference and a pin switch matrix. The ADuCM350 has a six-button CapTouch interface that is connected via a capacitive sensor using self capacitance measurements. This CapTouch interface supports a low power mode. It also integrate other noise reduction techniques, making it potent to environmental conditions [48] [32]. ADuCM350 evaluation board is shown on figure 24 below.

3.1.1 Arm cortex-m3 on aducm350

The ADuCM350 is build in with the complete embedded trace of the ARM Cortex-M3 processor features in order to maximize the code analysis, system profiling and debugging capabilities. Cortex-M3 processor is an ARM processor for low cost embedded systems targeted at ultralow power processing and delivering other high performance features that is expected from an ARM core in the memory footprint which is associated with 8-bit and 16-bit devices[49] . Section 3.1 describes some features of Arm cortex-M3.

Examples of Arm cortex-M3 processor includes, a low gate count processor core, with low latency interrupt processing, nested vectored interrupt controller (NVIC) which is integrated with the processor core to achieve low latency interrupt processing, memory protection unit (MPU) which is an optional MPU for memory protection, bus interfaces and low-cost debug (example includes serial wire JTAG debug port, optional data watchpoint and trace (DWT) and others).

3.1.2 Software development kit and installations

As eailer stated ADuCM350 software development kit (SDK) is only suppoerted by the IAR embedded workbench for ARM (EWARM) cortex-M tool chain. The evaluation kit is designed specifically to work with the ADuCM350 SDK and the evaluation kit support package (EKSP), both of which are available for download on the ADuCM350 design for free. The ADuCM350 evaluation kit provides researchers, system analyzers, and software developers a platform to drift from sensor investigation and analysis to full ecosystem development. The evaluation kit consists of an ADuCM350 motherboard and a selection of analog front end and digital peripheral daughter boards as shown in figure 23 [47][48][49].
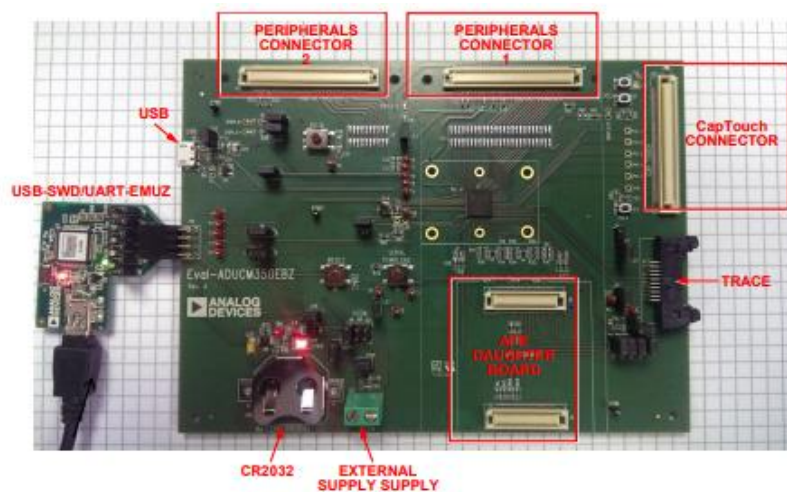
Figure 23. AduCM350 Evalution Board Typical Setup [49].

Steps to follow for software installation. First download and install the IAR embedded workbench environment for cortex-M (EWARM). Secondly, download and install the latest ADuCM350 SDK. Finally, download the PC driver required for the USB/UART emulator board. The required J-Link driver software for the J-Link OB which can be obtained from segger sites because they are the manufacturers. The reason for this order of installation is that, the ADuCM350 SDK installer will install some important configuration files into the EWARM directory. If the SDK is install before EWARM, the IDE will not be able to find these files which will result to build-time errors. EWARM should be installed before the SDK.

3.1.2.1   J-Link ob connector

The J-Link OB emulator enables nonintrusive emulation via a serial wire which allows supply and SPI, I2C, UART or I2S communications with the ADuCM350 evaluation board. Figure 24 above shows an example of how the emulator is connect to the ADuCM350 evaluation board. Some of it features are debugging support and download into the flash memory. It is use for testing and debugging the target device, typically a microcontroller.

3.1.3 Security integrity of the aducm350

ADuCM350 is designed with various features to address the issue of security with the following three goals.

> ➢ To ensure that the device conditions are suitable for code execution.
> ➢ To prevent unauthorized access or copying of user code.
> ➢   To prevent tampering of a device with the intention of altering its intended use

 The application of the above mention goals further outlines other features such as the initialization, authentication, real-time checking, JTAG/serial wire, flash, failure analysis, and serial downloader features [50]. These features are developed on the ADuCM350 microcontroller to make the device more secured for the end-users.

3.1.4 Aducm350 measurement

Using the ADuCM350 as the measurement hub and the AD8232 series, it is possible to perform both bio-impedance and ECG measurements with one solution. Chapter 4 of this thesis describes the possibilities with demonstrated examples.

Some of the features of ADuCM350 is the ability to perform a complex impedance measurement engine based on 2048-point, discrete fourier transform (DFT) and single frequency. The microcontroller takes the 16-bit ADC output as an input and gives an outputs of a real and imaginary parts of the complex impedance. ADuCM350 provide three different configurations for measuring the impedance of a sensor which are 2-wire system, 4-wire system and 4-wire bio-isolated system [51].

The 2-wire system is use to measure the relative accuracy of impedance magnitude and phase. This is because of the of varying access resistance of the unknown impedance.

The configuration provides relative accuracy measurements for impedance magnitude and impedance phase. In 4-wire system configurations the access resistance are calibrated out, this provides absolute accuracy for both impedance magnitude and impedance phase measurements, although isolation capacitors are not allowed. The 4-wire system configuration does not operate where AC coupling capacitors are required to isolate a sensor from the device, the capacitors are in series with the access resistances. The 4-wire bioisolated system, is use to measures the absolute accuracy of impedance magnitude in the presence of isolation capacitors and an external amplifier is needed to measure the differential voltage across the sensor. In this configurations, the system is not targeted for accurate phase measurements. The ADuCM350 alone is not able to do the measurement as a single chip because the isolated capacitors cause instability when included on the sense path [51][52].

After obtaining the current and voltage DFT measurements, the device can exit the AFE sequencer and calculate the impedance of the sensor using the following equations:

$$Voltage/Current Measurement\ Magnitude = \sqrt{r^2 + i^2} \tag{6}$$

$$Voltage/Current\ Measurement\ Phase = A * Tan(\frac{i}{r}) \tag{7}$$

where r and i are the real and imaginary components from the voltage and current DFT measurements, respectively. To calculate the Impedance Z, use Ohm's law by dividing the voltage magnitude by the current magnitude while taking into account the gains of the signal chain as follows:

$$Z_{Magnitude} = \frac{Voltage\ Magnitude}{Current\ Magnitude} \tag{8}$$

3.1.4.1   Impedance measurement in labview
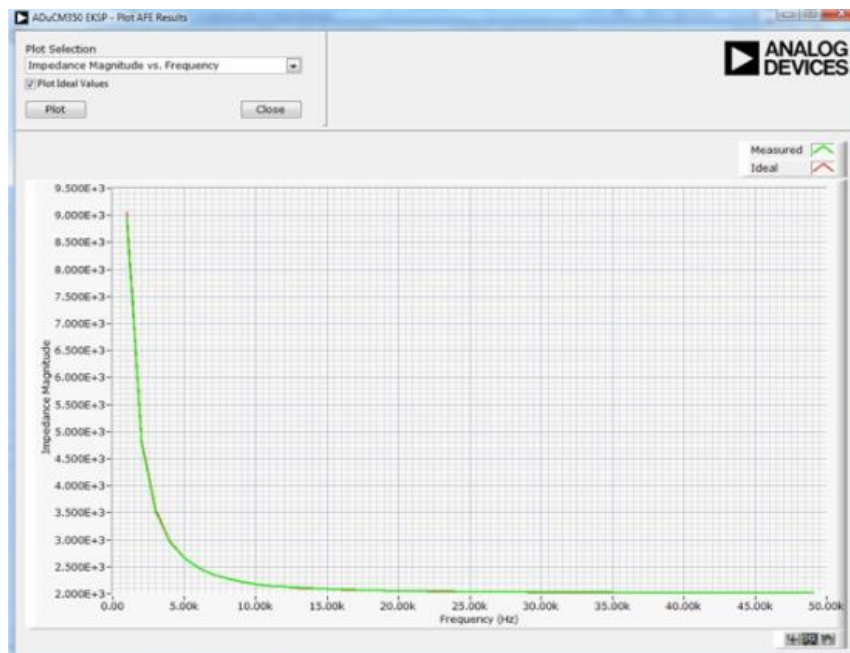
Figure 24. Measured Versus Theoretical Impedance Frequency Sweep [46].

Impedance and sensor measurements can be done with the ADuCM350 LabVIEW graphical user interface (GUI). The LabVIEW impedance measuring analog front end (AFE) control window is shown in Figure 25. The LabVIEW impedance measurement plot is shown in Figure 6 [46].

3.2 nRF8001 Bluetooth Chip

The nRF8001 is a Bluetooth low energy (BLE), this is designed to archeive operation in the peripheral (slave) role. nRF8001 integrates a BLE compliant radio (PHY), slave mode link controller, and a host which is usually a microcontroller. The nRF8001 offers a comprehensive method to add BLE connectivity to an application. It offers a serial interface for configuration and control by a microcontroller. nRF8001 is integrated with a non-volatile memory on-chip that is use for storing service configurations and it helps in reducing the requirements on the microcontroller that deals with handling of all real-time operations which are related to the BLE communication protocol. The BLE chip also, includes a power supply voltage monitor and a temperature sensor that reduces the requirements to the microcontroller. These features are attainable through the

Application Controller Interface (ACI) as shown in figure 26 below [48]. BLE nRF8001 can be use in applications such as sports and fitness sensors, healthcare and medical sensors, remote controls, watches, mobile phone peripherals, automation sensors and others.
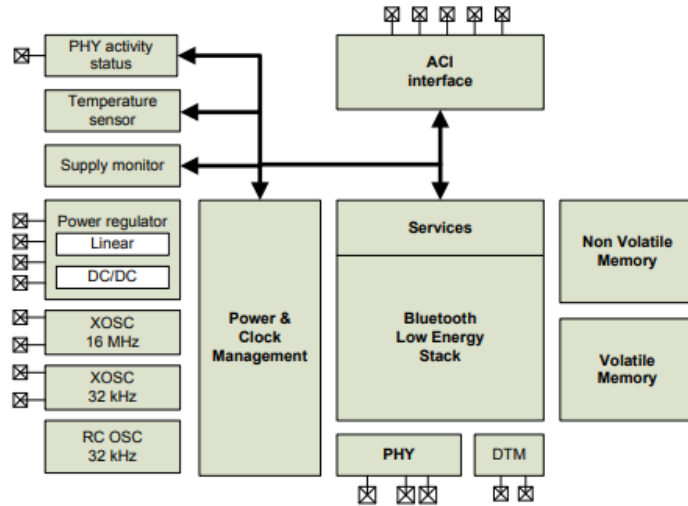
Figure 25. nRF8001 block diagram [53].

In figure 26 above, describes nRF8001's physical features such as the volatile and non volatile memory, BLE PHY and the BLE stack that handles the link controller and host stack. It also includes additional analog sub-systems needed for the BLE operation, such as power and clock management and other oscillator options.

nRF8001 features

- Radio features
  - *Bluetooth* low energy RF transceiver
  - Ultra-low peak current consumption <14 mA
  - Common TX/RX terminals
  - Low current for connection oriented profiles, typically 2 µA
  - Ultra-low current for connectionless oriented profiles, typically 500 nA
- Auxiliary features
  - Integrated low frequency reference oscillator
  - Power management
  - Battery monitor
  - Temperature monitor
  - DC/DC converter that reduces current by up to 20% if enabled
  - Integrated 16 MHz crystal oscillator
  - OTP for customer configuration
- Interfaces
  - UART Test Interface for Direct Test Mode
  - Application Controller Interface (ACI)
  - Radio Active signal

Bluetooth low energy features

- *Bluetooth* low energy stack
  - All layers up to GATT included in core software stack
- Link Layer Features
  - Slave role
  - Control PDUs in the slave role
  - 27 byte MTU
  - Encryption
- L2CAP
  - 27 byte MTU
  - Slave connection update
  - Attribute Channel
  - Security Channel
- General Access Profile (GAP) features
  - Discoverable modes
  - Dedicated bonding
  - GAP attributes
- Attribute Protocol
  - Mandatory client protocol
  - Mandatory server protocol
- Security Manager
  - Generation of keys for encryption
  - Just works security
  - Passkey entry
- Generic Attribute Profile (GATT)
  - Mandatory client profile features
  - Mandatory server profile features
- Direct Test Mode (DTM)
  - DTM for RF qualification

Figure 26. nRF8001 BLE features [53].

Figure 26 above gives the BLE nRF8001 key features. nRF8001 is designed to be used in together with an external microcontroller that is running the application. The nRF8001 integrates a PHY, link controller and host single mode BLE subsystem and features a communication protocol such as SPI, which can be interface with a microcontroller application. nRF8001 also, includes analog features such as BLE RF transceiver, three on-chip oscillators, DC/DC converter for extended battery life with coin-cell batteries, temperature sensor and battery monitor.

3.2.1 nrf8001 application controller interface (ACI)

The function of an application controller interface (ACI) is to enables a microcontroller to communicate with the BLE nRF8001. The ACI on nRF8001 have five output pins MISO, MOSI SCLK, Ready (RDYN) and Request (REQN). Both RDYN and REQN permits the nRF8001 to notifications to the microcontroller, when it has received new data over-the-air and also to hold new data exchanges initiated by the microcontroller until the microcontroller is ready to accept and process them. The microcontroller must always, have the RDYN configured as input with pull-up drivers. This is because at power on reset and wake up from sleeping mode, the RDYN level is valid after about 62 ms from reset or wake up mode. The ACI connections are described in figure 27 below. All data exchanges in ACI uses SPI interface, with the nRF8001 using slave mode 0 interface to

the microcontroller as its communication protocol. The nRF8001 behaviour does not distinguish it as a pure SPI slave device. This is because nRF8001 can receive new data over-the-air at any given time or it would be processing a connection event.
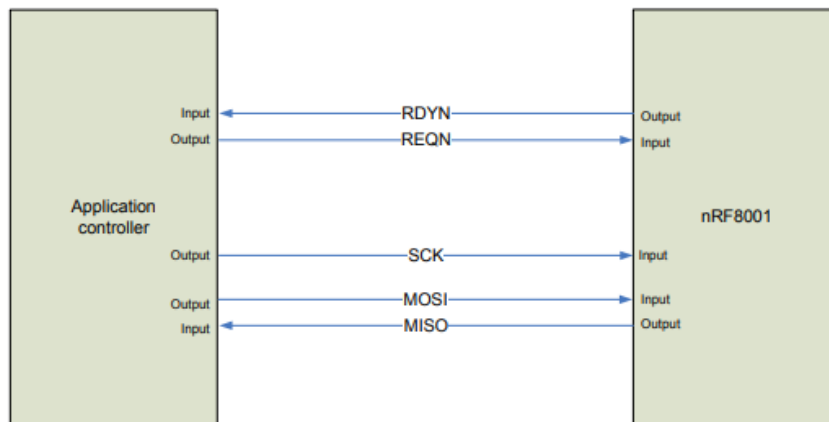
Figure 27. ACI interface between application nRF8001 and microcontroller [53].

Data exchanges on the ACI interface are divided into two types the commands and events. The commands exchanges are initiated by the microcontroller which include data that is sent from the microcontroller to nRF8001 while events exchanges are initiated by nRF8001, these include data that is sent from nRF8001 to the microcontroller. If the nRF8001 BLE has an event data that is ready for the microcontroller and when the processor requests a command exchange, both the command and event will be combined to form a full duplex exchange as shown in figure 29. The nRF8001 is capable of sending out the event data and receiving command data at the same time. In order to accomplish this, the microcontroller must always monitor the incoming data when issuing a command [53].

3.2.2 Sending and recieving data in nrf8001

As discussed in sub-section 3.2.1, nRF8001 ACI communication protocol transport layer uses the SPI in mode 0. Table 2 below gives the SPI signal description.

Tabel 3 SPI description [53].

Type	Value
Data Order	Least significant bit first

Clock Polarity	Zero (base value for the clock is zero)
Clock Phase	Zero (data is read on the clock's rising edge)
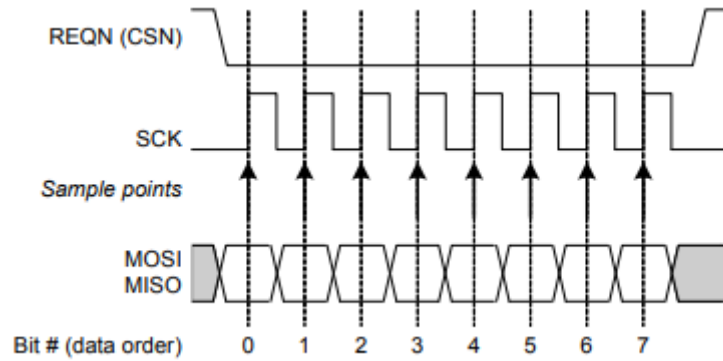
Figure 28. SPI mode 0 description [53].

Figure 29 above shown the SPI mode 0. In this mode, the clock polarity is 0, which indicates that the idle state of the clock signal is low. The clock phase in this mode is 0, which indicates that the data sampled on rising edge and shifted out on the falling edge. Figure 29 below shows the signaling in an ACI command sent from a microcontroller to nRF8001 and signaling in an ACI event exchange from nRF8001 to the microcontroller.
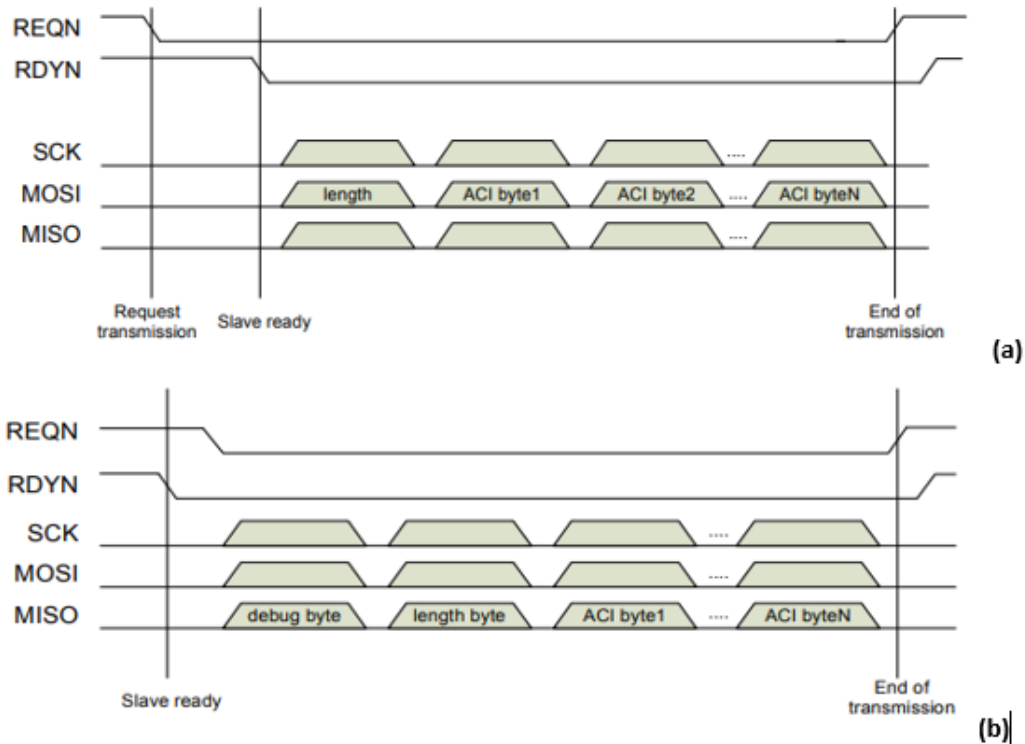
Figure 29. (a) Data exchange from a microcontroller to nRF8001 and (b) Receiving an ACI event from nRF8001 [53].

Some procedures needed to be perform when the microcontroller sends a command to nRF8001 as shown in figure 30a above such as the microcontroller requests the right to send data by setting the REQN pin to ground, the nRF8001 sets RDYN pin to ground when it is proceeding to receive data and finally the microcontroller starts sending data on the MOSI pin as describe by the length. Also, the following procedures are performed as shown in figure 30b by the microcontroller when it receives the ACI event such as the nRF8001 sets the RDYN pin to ground, the microcontroller sets the REQN pin to ground and starts clocking on the SCK pin according to the length of byte describe and finally the microcontroller sets the REQN pin high to close the event. The command packet's maximum length is 32 bytes while the maximum length of an event packet is 31 bytes. The nRF8001 has the ability of receiving an ACI command and at the same time is able to send an ACI event to the microcontroller known as the full duples ACI transaction [53].

3.2.2.1 Data Storage in nRF8001

nRF8001 store data in either volatile or non-volatile memory, this depends on the type of data store. The data is classified into two static and dynamic data. Static data in

nRF8001 is configured through the ACI to hold both hardware and protocol parameters. This setup data is written to non-volatile memory for permanent storage or to volatile memory during application development. In dynamic data, during runtime operation, the nRF8001 application will contain the attributes and acquire information about other peer devices and the services they offer. The runtime application will establish a bond connectivity with a new peer device. The information that the application gets from a new peer device during the runtime operation, is stored in nRF8001 as volatile memory known as dynamic data [53].

3.3 Other Micro chips Integrated in the Project

3.3.1 ADS7946 analog to digital converter

ADS7946 is a 14-bit, 2 Megasamples per second (MSPS) analog to digital converter, that has a single ended input. This device has a 16 clock data frame operating at a sample rate of 2 MSPS. It features an oustanding dc precision with an excellent dynamic performance. The ADC has an integrated 2-channel multiplexer and a sucessive aproximation register (SAR). This device communicates over the serial peripheral interface (SPI) [54].

In this project, the ADC takes it input from sensors in the form of impedance/voltage and converts it to digital formats (bits) which is then interfaced with the microcontroller for further processing and analysis.

3.3.2 ICM-20948

The ICM-20948 is an extremely low powered, SPI and I2C enabled 9-axis motion tracking device that is perfectly suited for smartphones, wearable sensors, tablets and IoT applications. It boasts of a 3-axis gyroscope, 3-axis accelerometer, 3-axis compass and a digital motion processesor. It also has an on-chip 16-bit ADC and programmable filters [54].

3.3.3 SPO2 sensor max30101 efd+

The MAX30101 is an integrated heart rate and pulse oximetry monitor module used for fitness and healthcare. The device consists of internal LEDs, optical element, photodetectors, and low-noise electronic that has ambient light rejection. MAX30101 operates with on two power supply, the first is a 1.8V that power the device while a separate 5.0V power supply powers the internal LEDs. The device communicates with the microcontroller through a I2C compatible interface. The module has the capability of being shut down via software with a zero-current consumption on standby. Its application is typically found in fitness assistant and wearable devices [55].

4 Hardware and Software Implementations

4.1 Hardware Implementation

The main aim of the implementation is for the ADuCM350 to get data from the sensors and then transmit them via the nRF8001 Bluetooth module to a smartphone where the raw data can be viewed. The ADuCM350 communicates with the nRF8001 via the Serial Peripheral Interface (SPI0), while the nRF8001 sends the data via a protocol known as "Bluetooth over UART", meaning a UART connection is being transmitted over Bluetooth. The whole setup is on a prototype board and it is powered by an adjustable DC-DC converter which outputs 5 volts DC. Code is flashed from a Windows PC to the ADuCM350 using a Segger J-link adapter which is a USB-to-Serial device. Extra input and output pins are available on the board for the connection of other peripherals for example sensors (ECG, SPO_2), and via which the processor can be debugged.

4.1.1 ADuCM350 Development Board
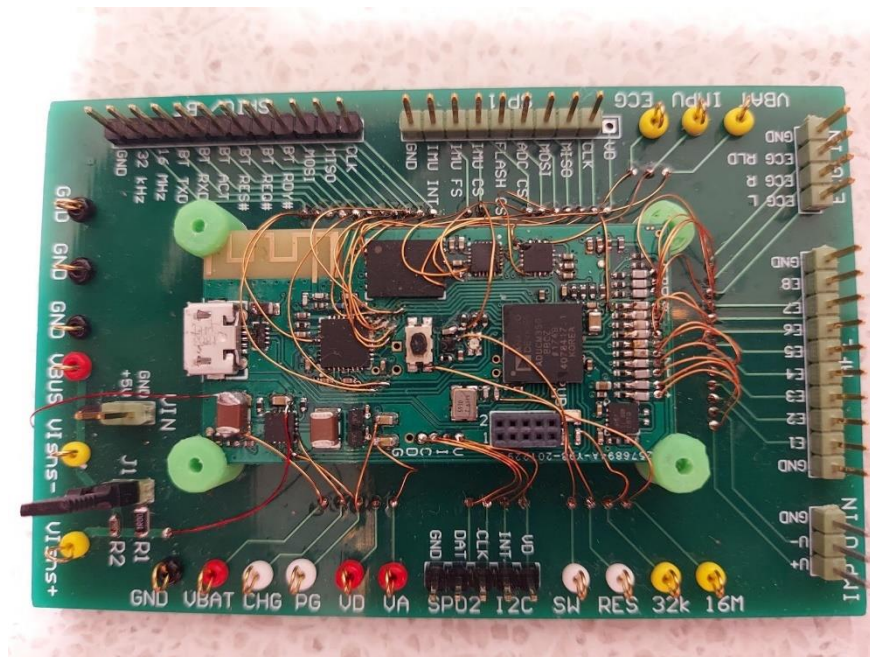
Figure 30. The ADuCM350 Developmental Board.

The ADuCM350 development board runs at approximately 5 volts DC which is supplied by the DC-DC converter, and it draws an average current of 110mA.

Figure 31. Segger J-link

It is used to download code to the flash memory of the ADuCM350, and also to debug code and troubleshoot the microcontroller. J-Link is used in this project because of its ability to support directly interfacing SPI flashes between CPU and the SPI.

Figure 32. DC-DC Converter.
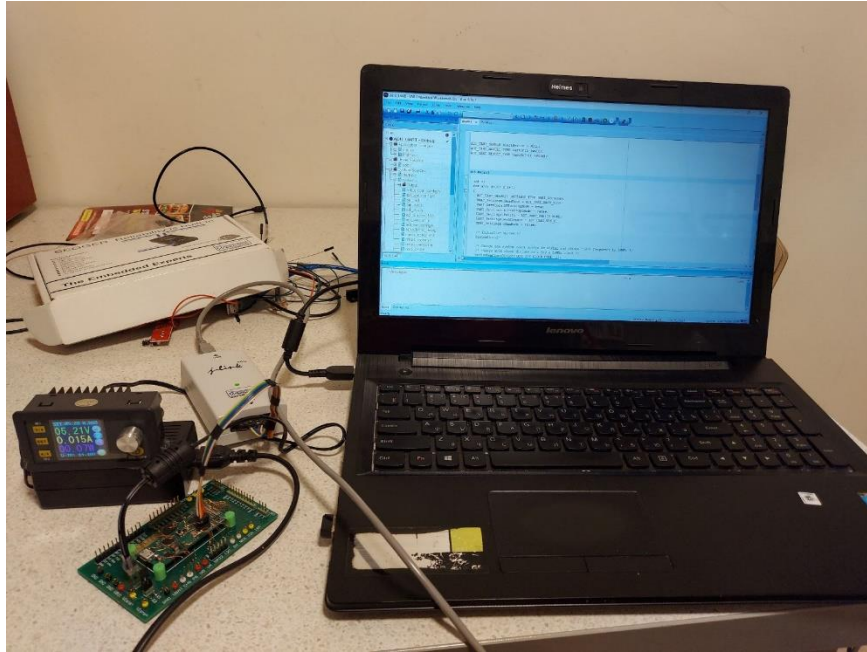
Figure 33. System setup.

This is just a typical set up as described in section 4.1. The microcontroller is connected to the computer via segger J-link and it is power on by the dc-dc converter.

4.2 Software Implementation

4.2.1 General overview of the software archtecture

The ADuCM350 is a microprocessor that is based on ARM Cortex M3 architecture. It runs on code written in C/C++, and it stores the files and libraries needed by the nRF8001 to function. The ADuCM350 interfaces with nRF8001 in the embedded software program that is written in this project. The ADuCM350 gets data from the sensors (ECG, SPO2) and passes it to the nRF8001 Bluetooth, while the Bluetooth will broadcast to a nearby connected channel (mobile phone) over UART or stores the data in the external memory where there are no connections. Software Environment

The ADuCM350 board code is written with the "IAR Embedded Workbench for ARM" IDE from IAR Systems. The written code is transmitted to the board via the Segger J-link device which converts the USB interface to Serial.

4.2.2 Software environment

The ADuCM350 board code is written with the "IAR Embedded Workbench for ARM" IDE from IAR Systems. The written code is transmitted to the board via the Segger J-link device which converts the USB interface to Serial.

4.2.3 Embedded programing

The ADuCM350 has a Software Development Kit (SDK) that can be downloaded from the Analog Devices website. It possesses drivers needed for the chip to work, and, also example code which serve as a base or template for developing new code. The SDK is compatible with IAR Embedded Workbench out of the box.

The nRF8001 also has an SDK which can be downloaded from the Nordic Semiconductors Github repositories, but it is not directly compatible with the ARM Cortex M3 platform because it was written for Arduino. It had to be ported to the Cortex M3 platform using nRF go Studio after which the IAR Embedded Workbench recognized it.

4.2.4 Interfacing aducm350 and nrf8001 micro chips

The ADuCM350 and the nRF8001 communicate via the Serial Peripheral Interface. The ADuCM350 uses the SPI0 port which includes the SCK, MISO, MOSI, and CS pins. The nRF8001 also has these pins, but it has some extra pins which are RDYN, REQ, and RES. The functions of the pins are described below:

- SCK, which is short for 'Serial Clock', is the line used to set the frequency or baud rate at which the SPI operates. It sets it for both the master and slave devices and is connected across them. In this setup, the ADuCM350 is the master device.
- MISO, short for Master in Slave Out, is the line on which the slave device sends data to the master device.
- MOSI, short for Master Out Slave In, is the line on which the master device sends data to the slave device.
- CS, short for Chip Select, is the pin on which the target slave device is selected. The identifiers are defined in the code hosted on the master device, in this case the ADuCM350, and it allows for multiple slave devices to be put on the same SPI port.
- RDYN is a digital output pin used to indicate to the microcontroller that the device is ready to perform a task.
- RES is a digital input pin used to reset the nRF8001 module.

- REQ is a digital input pin used to make requests to the nRF8001 module.

4.2.5 How the code works

The ADuCM350 starts up and initialises the SPI interface which also initialises the nRF8001 chip which returns a signal through the RDYN pin to state that it is active. When the ADuCM350 chip gets signals from the attached sensors, it processes them to get raw data, then it sends the data to the nRF8001 via the SPI0 port. To signal that data is inbound the nRF8001 chip, it toggles the REQ pin to perform a handshake which then allows the data to be received on it. After this, the nRF8001 then sends the received data to a connected smartphone via a protocol known as "UART-over-Bluetooth" which is able to serve a UART connection over bluetooth. The parameters of connection and operation are set in the nRF8001 libraries already imported on the code, and the code resides in the flash memory of the ADuCM350.

5 Results

I tested the board with a DHT11 sensor from Adafruit, and the results were displayed real-time on the nRF Connect app, and also Bluefruit Connect app running on three different smartphones. I tested it on multiple devices and apps to ensure compatibility. I took out only the temperature data in Celsius and transmitted it. The screenshots can be seen below with timestamps.
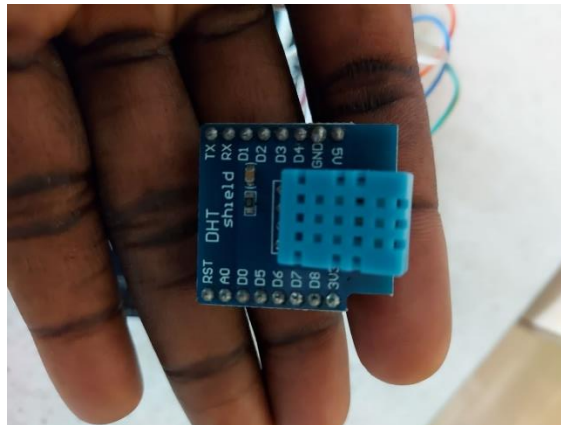
Figure 34. Temperature Sensors
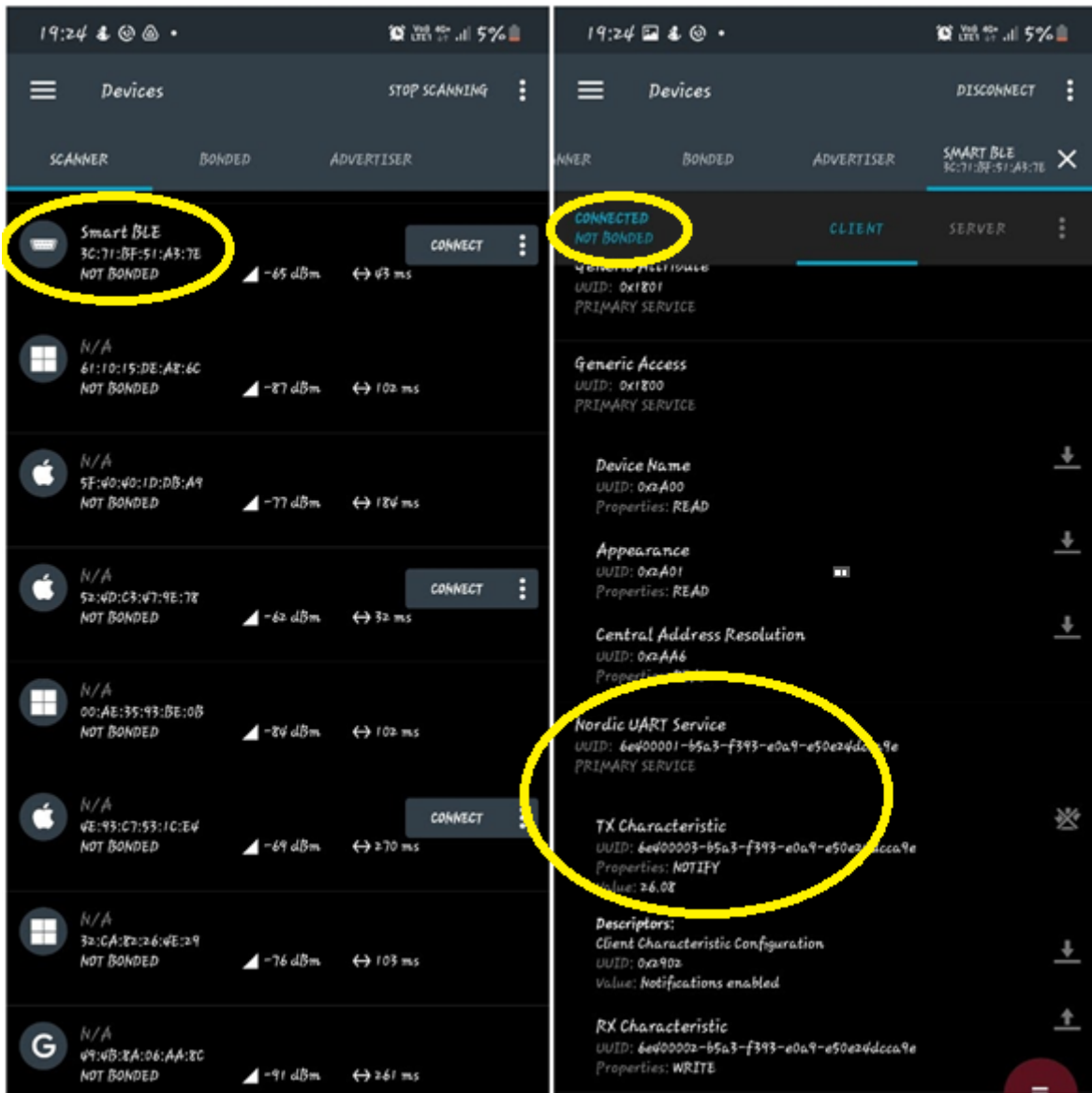
Figure 35. nRF Connect on a Samsung Galaxy S10 Lite SM-G770F/DS running Android 11

The figure above show the connectivity between the nRF8001 Bluetooth and nRF Connect app running on running Android 11 displaying the data sent from the microcontroller.
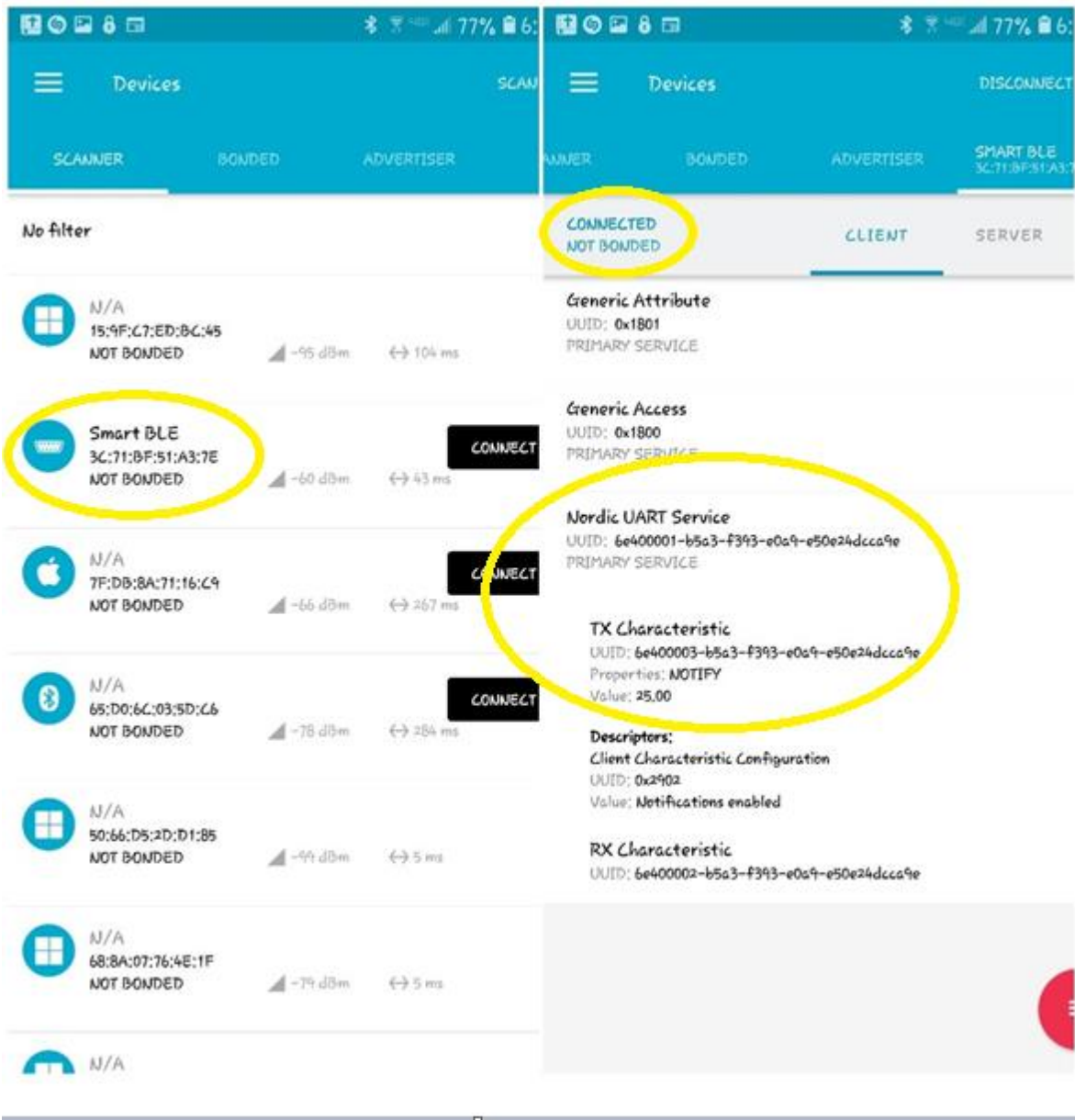
Figure 36. nRF Connect on a Samsung Galaxy S7 Edge SM-G935V running Android 8.0.0

The figure above show the connectivity between the nRF8001 Bluetooth and nRF Connect app running on running Android 8.0.0 displaying the data sent from the microcontroller.
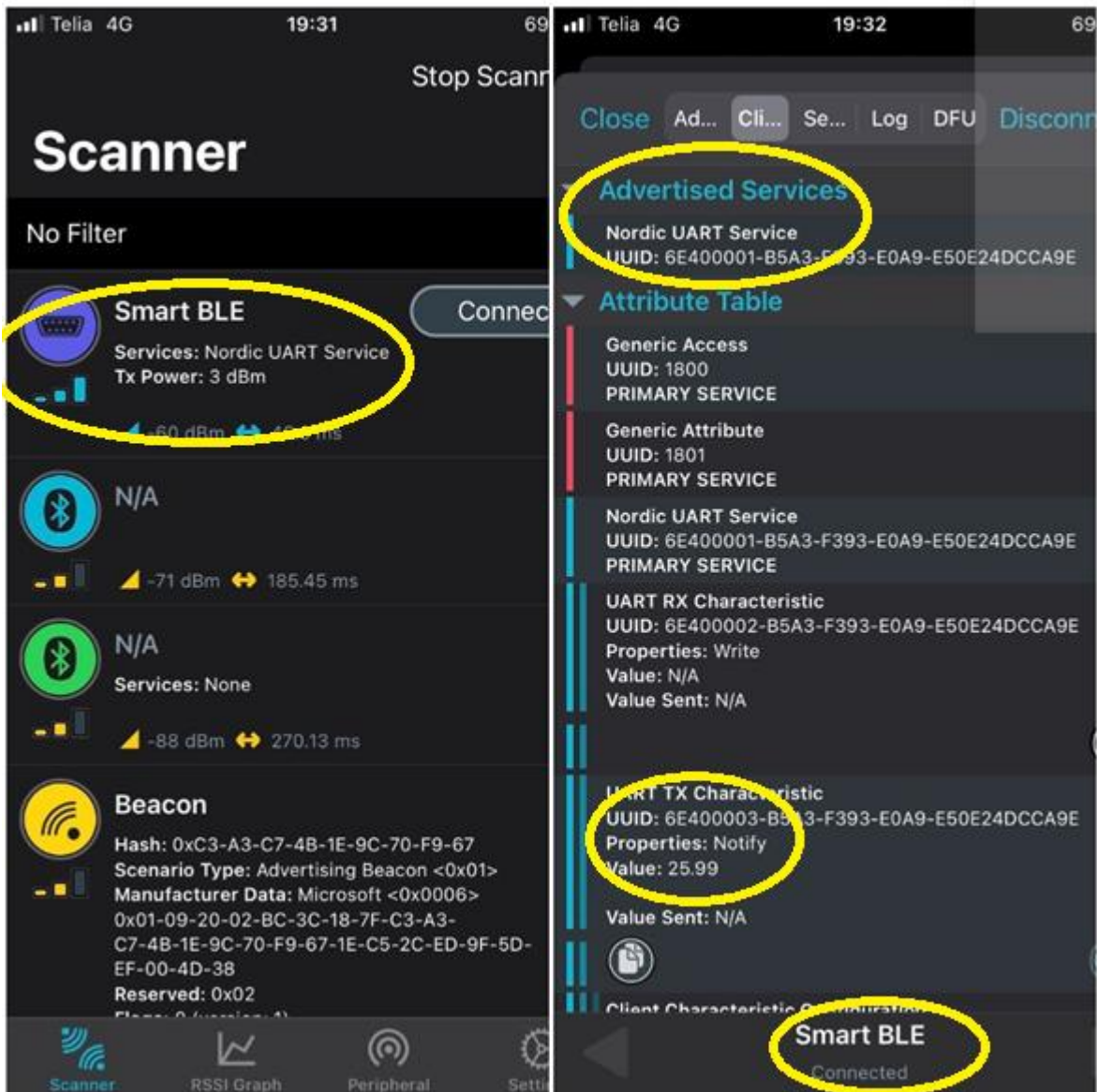
Figure 37. nRF Connect on an iPhone 8 running iOS 14.4.2

The figure above show the connectivity between the nRF8001 Bluetooth and nRF Connect app running on running on iOS 14.4.2 displaying the data sent from the microcontroller.
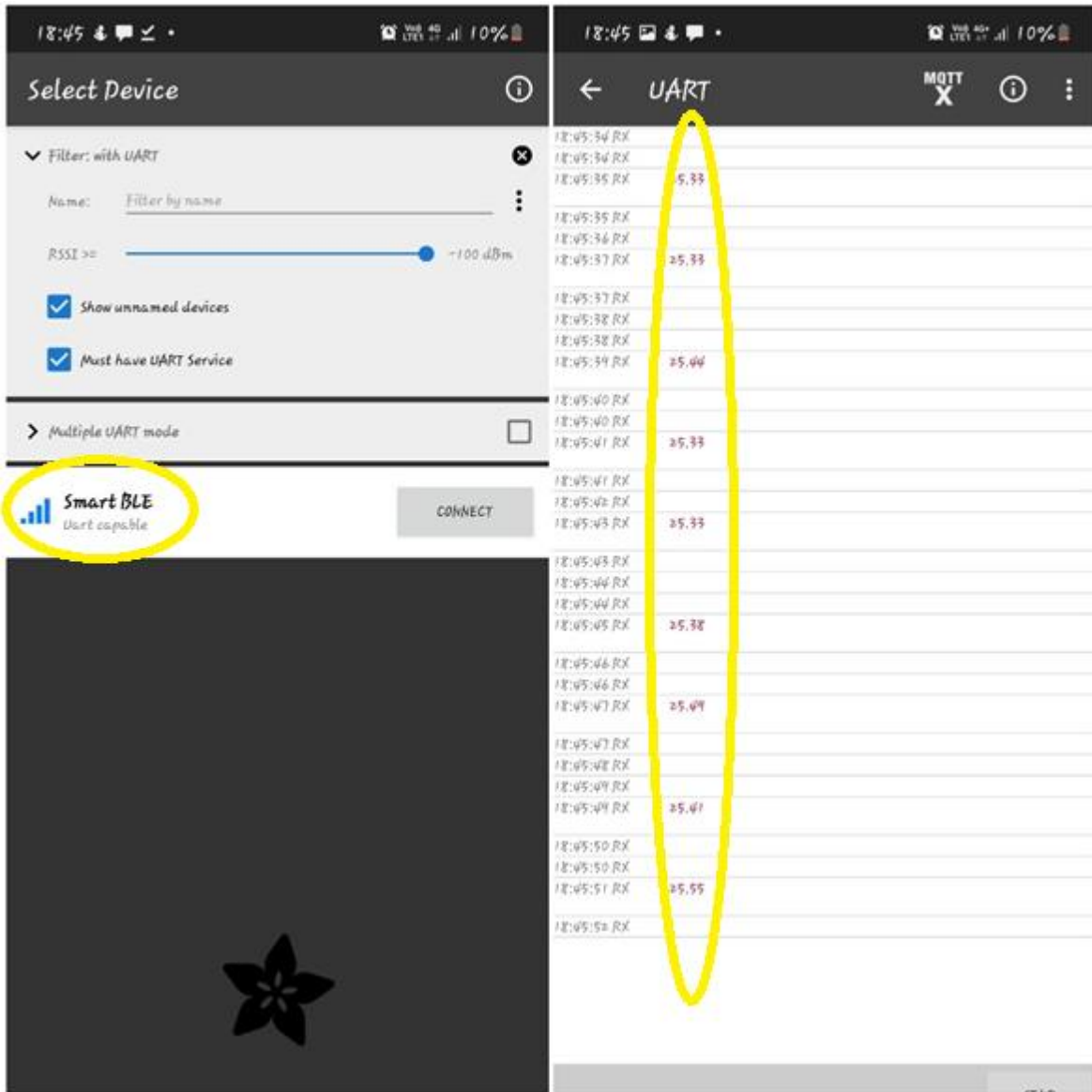
Figure 38. Bluefruit Connect on a Samsung Galaxy S10 Lite SM-G770F/DS running Android 11.

The figure above show the connectivity between the nRF8001 Bluetooth and Bluefruit Connect running on running Android 11 displaying the data sent from the microcontroller.

Figure 39. Bluefruit Connect on a Samsung Galaxy S7 Edge SM-G935V running Android 8.0.0

The figure above show the connectivity between the nRF8001 Bluetooth and Bluefruit Connect app running on running Android 8.0.0 displaying the data sent from the microcontroller.
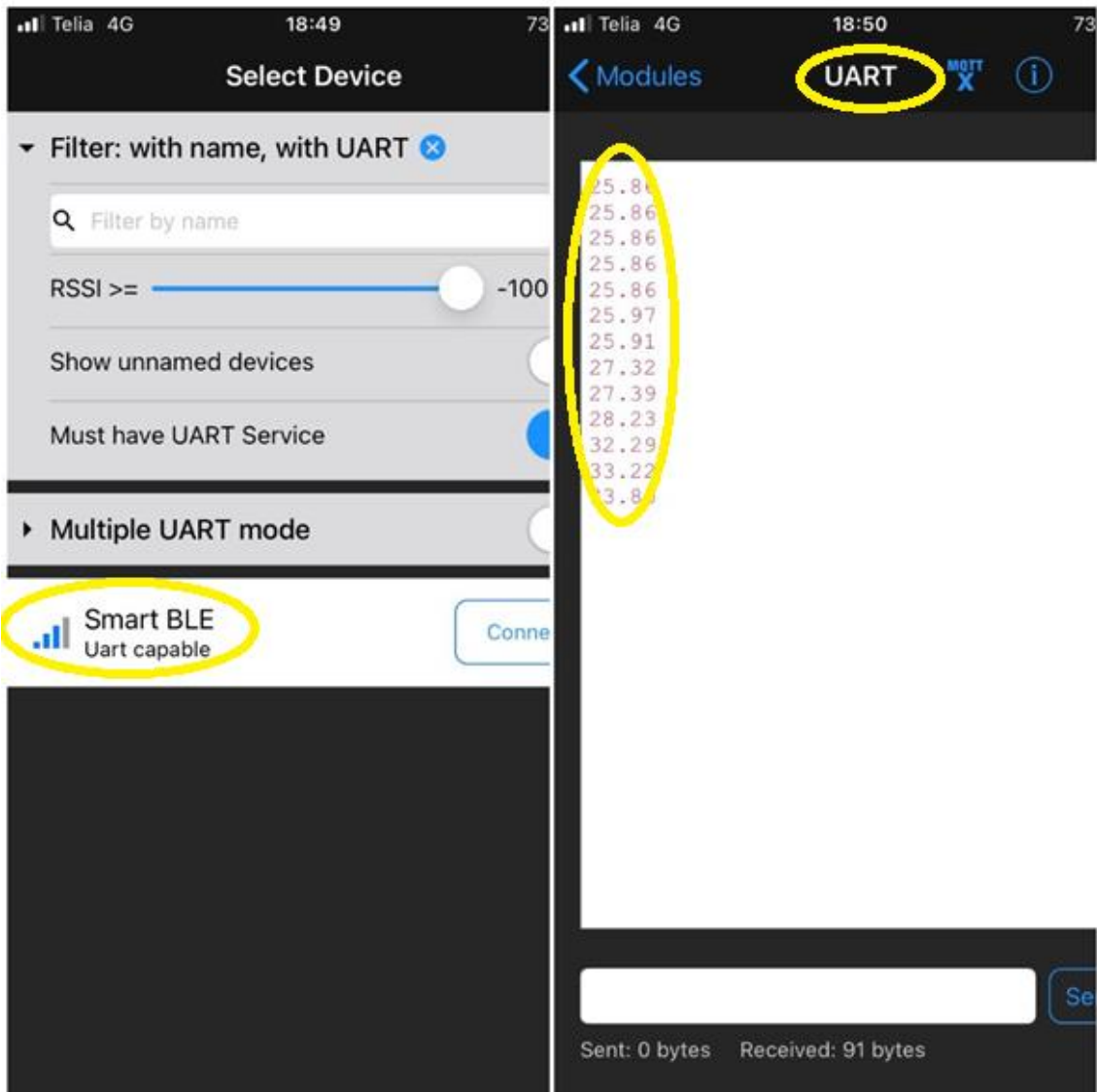
Figure 40. Bluefruit Connect on an iPhone 8 running iOS 14.4.2.

The figure above show the connectivity between the nRF8001 Bluetooth and Bluefruit Connect app running on running Android 8.0.0 displaying the data sent from the microcontroller. I set the delay in transmission to 2000 milliseconds to give enough time for noticing changes in the data, and I set the Bluetooth UART to check data availability every 100 milliseconds. The setup can be used to display data from any sensor or peripheral device attached to the board.

6 Conclusion

The aim of this thesis is to develop an embedded software program and interface ADuCM350 with nRF8001 Bluetooth for the measurement of physiological vital signs (mainly ECG, SPO_2) that is discussed in this thesis. The task to develop the embedded firmware driver for the NRF8001 module and the impedance based peripherals of the ADUCM350 microcontroller, has been achieved as displayed in the results in chapter 5. The microcontroller is able ready and send information to the Bluetooth and the Bluetooth I to transmit it over UART and the results is displayed. There were many challenges, and this comes from the lack of resources from the chip manufacturer. However, these challenges were overcome.

I will recommend the ADuCM350 to be replaced by an ATmega328P or ATmega2560 or STM32 based MCU with good online support and software resources. This is since the ADUcM350 has almost no support online so programming it is a very difficult task, unlike other microcontrollers.

The nRF8001 should be replaced with an ESP32 module. The nRF8001 works, but it's old and the ESP32 is newer and has way more support. The ESP32 also has WiFi and can also be used as an access point or a websocket, or it can upload data directly to a configured server.

The IAR workbench does not support many libraries out of the box and they have to be rewritten for them to work. This is a very stressful and time-consuming step because some libraries are over 7,000 lines of code.

6.1 JÄRELDUSED

Selle lõputöö eesmärk on välja töötada sisseehitatud tarkvaraprogramm ja liides ADuCM350 koos nRF8001 Bluetoothiga füsioloogiliste elutähiste (peamiselt EKG, SPO2) mõõtmiseks, mida käesolevas töös käsitletakse. NRF8001 mooduli sisseehitatud püsivara draiveri ja mikrokontrolleri ADUCM350 impedantsil põhinevate välisseadmete väljatöötamise ülesanne on täidetud, nagu on näidatud peatüki 5 tulemustes. Mikrokontroller suudab Bluetooth-i ja Bluetooth I-le teavet valmistada ja teavet saata. edastage see UART-i kaudu ja tulemused kuvatakse. Väljakutseid oli palju ja see tuleneb kiibitootja ressursside puudumisest. Nendest väljakutsetest sai siiski üle.

Soovitan ADuCM350 asendada hea veebitoe ja tarkvararessurssidega ATmega328P või ATmega2560 või STM32 põhise MCU-ga. Seda seetõttu, et ADUcM350-l pole veebis peaaegu mingit tuge, seega on selle programmeerimine erinevalt teistest mikrokontrolleritest väga keeruline ülesanne.

NRF8001 tuleks asendada ESP32 mooduliga. NRF8001 töötab, kuid see on vana ja ESP32 on uuem ning sellel on palju rohkem tuge. ESP32-l on ka WiFi ja seda saab kasutada ka pöörduspunktina või veebipesana või laadida andmeid otse seadistatud serverisse.

IAR-i töölaud ei toeta paljusid raamatukogusid karbist välja ja need tuleb tööks ümber kirjutada. See on väga pingeline ja aeganõudev samm, sest mõnes raamatukogus on üle 7000 koodirea.

Summary

Every year, millions of people die as a result of cardiovascular diseases. Fatalities can be avoided by using early detection and pervasive monitoring. Wearable technology advancements are assisting in achieving better control of the state of the health of the cardiac patients. The aim of this thesis is to create an embedded software program for the wearable cardiovascular monitor which is using analog front-end chip ADuCM350 and nRF8001 Bluetooth chip for connectivity. This wearable device will measure important vital parameters and will send the information over Bluetooth to various devices (mobile phone). Heart rate, blood saturation (SPO2), and an electrocardiogram are all indicators of state of the cardiovascular system and will be measured by the device. The ability to capture the vital parameters wirelessly and send them to predetermine destinations adds to the power of enhancing care management. Data protection and regulatory approval are two issues that wearable devices face. A few suggestions to overcome the challenges are discussed. In conclusion, the use of wearable monitors allows for improved cardiac patient monitoring and contact with physicians, resulting in more efficient care management.

In this thesis, a wristwatch-like wearable Bluetooth device for monitoring and collecting data of physiological (ECG and SPO2) has been proposed with a prototype. The data collected from this wearable device will be sent over Bluetooth to a different system (smartphone) that is later analyzed. The task of this thesis is to develop an embedded firmware driver for the NRF8001 module and the impedance based peripherals of the ADUCM350 microcontroller. The ADUCM350 has a low user base and less resources, hence, increases the complexity of the project. Our goal is to create a prototype based on the custom embedded firmware to be developed utilizing the onboard impedance measuring peripheral and the other physiological signals based sensors onboard.

The outcome of this thesis is that the embedded firmware drivers have been developed and tested. The ADuCM350 microcontroller is able to communicate with nRF8001 Bluetooth by sending some data to it, while the nRF8001 Bluetooth receives the data. The nRF8001 Bluetooth transmits the received data to a smartphone over UART. Two different applications were used for testing by the smartphone to receive data namely nRF Connect and Bluefruit Connect application downloaded from both iOS and Android application store. The results have shown that both iOS and Android devices are compatible with the developed firmware.

Kokkuvõte

Igal aastal surevad miljonid inimesed südame-veresoonkonna haigustesse. Surmajuhtumeid on võimalik vältida, kasutades varajast avastamist ja pidevjälgimist. Kantava tehnoloogia areng aitab kaasa südamehaigete tervisliku seisundi paremale jälgimisele.

Selle lõputöö eesmärk on luua tarkvara kaasaskantava kardiovaskulaarse monitori jaoks, mis kasutab mõõtmiseks kiipi ADuCM350 ja ühenduse loomiseks kiipi nRF8001. See kantav seade mõõdab olulisi parameetreid ja saadab teabe Bluetoothi kaudu erinevatele seadmetele (mobiiltelefon). Südame löögisagedus, vere küllastus hapnikuga (SPO2) ja elektrokardiogramm on kõik kardiovaskulaarsüsteemi seisundi näitajad ja neid mõõdab ka antud seade. Võimalus elutähtsaid parameetreid juhtmevabalt hõivata ja eelnevalt määratud sihtkohtadesse saata parendab patsientide jälgimist ja hoolduse korraldust. Andmekaitse ja regulatiivne heakskiit on kaks küsimust, millega kantavad seadmed silmitsi seisavad. Vaadeldakse mõningaid ettepanekuid väljakutsetest ülesaamiseks. Kokkuvõtteks võib öelda, et kantavate monitoride kasutamine võimaldab südamehaigete paremat jälgimist ja paremat kontakti arstidega, mille tulemuseks on tõhusam ravi ja hoolduse juhtimine.

Selles töös on teostusnäitena pakutud välja käekellataoline kantav Bluetooth-seade füsioloogiliste andmete (EKG ja SPO2) hõivamiseks, jälgimiseks ja kogumiseks. Sellest kantavast seadmest kogutud andmed saadetakse Bluetoothi kanali kaudu teise süsteemi (nutitelefoni), kus neid hiljem analüüsitakse. Üks lõputöö ülesandeid oli kirjutada NRF8001 mooduli jaoks tarkvara draiver mis võimaldaks ühendada ADUCM350 impedantsimõõtjat välisseadmetega. ADUCM350 ei ole veel väga levinud, tal on väike kasutajaskond ja veel vähe materjale millele toetuda, mis suurendab projekti keerukust. Eesmärk oli luua prototüüp, mis põhineb väljatöötataval kohandatud püsivaral ja kasutab erinevate füsioloogiliste signaalide hõivamiseks erinevaid sisseehitatud sensoreid.

Lõputöö tulemusena on valminud kohandatud püsivara ja see on ka testitud. Mikrokontroller ADuCM350 suudab suhelda nRF8001 Bluetoothiga, saates andmeid, samal ajal kui Bluetooth nRF8001 võtab andmed vastu. NRF8001 Bluetooth edastab vastuvõetud andmed omakorda nutitelefoni. Nutitelefonis kasutatakse andmete vastuvõtmiseks ja testimiseks kahte erinevat rakendust, nimelt nii iOS kui ka Androidi aplikatsioonipoest allalaaditud nRF Connect ja Bluefruit Connect rakendusi. Tulemusena on näidatud, et nii iOS- kui ka Android-seadmed on väljatöötatud püsivaraga ühilduvad.

LIST OF REFERENCES

[1]   L. Chaari Fourati and S. Said, "Remote Health Monitoring Systems Based on Bluetooth Low Energy (BLE) Communication Systems," in *The Impact of Digital Technologies on Public Health in Developed and Developing Countries*, Cham, 2020, pp. 41–54. doi: 10.1007/978-3-030-51517-1_4.

[2]   B. Noureddine and F. bereksi reguig, "Bluetooth Portable Device for ECG and Patient Motion Monitoring," *Nat. Technol. » Rev. Pages*, vol. 19, Feb. 2011.

[3]   T. M. Murray and S. M. Krishnan, "Medical Wearables for Monitoring Cardiovascular Disease," p. 8, 2018.

[4]   "Heart Disease and Stroke Statistics—2017 Update." https://www.ncbi.nlm.nih.gov/pmc/articles/PMC5408160/ (accessed Mar. 01, 2021).

[5]   J. J. Oresko *et al.*, "A Wearable Smartphone-Based Platform for Real-Time Cardiovascular Disease Detection Via Electrocardiogram Processing," *IEEE Trans. Inf. Technol. Biomed.*, vol. 14, no. 3, pp. 734–740, May 2010, doi: 10.1109/TITB.2010.2047865.

[6]   D. Dias and J. Paulo Silva Cunha, "Wearable Health Devices—Vital Sign Monitoring, Systems and Technologies," *Sensors*, vol. 18, no. 8, Jul. 2018, doi: 10.3390/s18082414.

[7]   Sverre Grimnes and Ørjan G Martinsen, *Bioimpedance and bioelectricity basics*, Third Edition vols. Boston, MA: Elsevier, 2014.

[8]   N. H. Kim and J. S. Ko, "Introduction of Wearable Device in Cardiovascular Field for Monitoring Arrhythmia," *Chonnam Med. J.*, vol. 57, no. 1, pp. 1–6, Jan. 2021, doi: 10.4068/cmj.2021.57.1.1.

[9]   J. Liu, M. Liu, Y. Bai, J. Zhang, H. Liu, and W. Zhu, "Recent Progress in Flexible Wearable Sensors for Vital Sign Monitoring," *Sensors*, vol. 20, no. 14, Art. no. 14, Jan. 2020, doi: 10.3390/s20144009.

[10]   F. Leu, C. Ko, I. You, K.-K. R. Choo, and C.-L. Ho, "A smartphone-based wearable sensors for monitoring real-time physiological data," *Comput. Electr. Eng.*, vol. 65, pp. 376–392, Jan. 2018, doi: 10.1016/j.compeleceng.2017.06.031.

[11]   "Wearable Technology Testing and Certification | UL."
https://www.ul.com/services/wearable-technology-testing-and-certification (accessed
May 11, 2021).

[12]   A. Ravizza, C. De Maria, L. Di Pietro, F. Sternini, A. L. Audenino, and C.
Bignardi, "Comprehensive Review on Current and Future Regulatory Requirements on
Wearable Sensors in Preclinical and Clinical Testing," *Front. Bioeng. Biotechnol.*, vol. 7,
Nov. 2019, doi: 10.3389/fbioe.2019.00313.

[13]   "Bluetooth and Beyond: Wireless Options for Medical Devices," *mddionline.com*,
Jun. 01, 2004. https://www.mddionline.com/news/bluetooth-and-beyond-wireless-
options-medical-devices (accessed May 12, 2021).

[14]   "How Lower Power Consumption is Transforming Wearables Battery Life."
https://valencell.com/blog/how-lower-power-consumption-is-transforming-wearables/
(accessed May 11, 2021).

[15]   C. Lockwood, T. Conroy-Hiller, and T. Page, "Vital signs," *JBI Libr. Syst. Rev.*,
vol. 2, no. 6, pp. 1–38, 2004, doi: 10.11124/01938924-200402060-00001.

[16]   "High Blood Pressure/Hypertension | Demo."
https://www.uhhospitals.org/sitecore/content/UHHospitals/Demo/Home/health-and-
wellness/health-and-wellness-library/article/adult-diseases-and-conditions-v0/high-
blood-pressurehypertension (accessed May 14, 2021).

[17]   "Understanding Blood Pressure Readings," *www.heart.org*.
https://www.heart.org/en/health-topics/high-blood-pressure/understanding-blood-
pressure-readings (accessed May 14, 2021).

[18]   J.-L. Vincent, "Understanding cardiac output," *Crit. Care*, vol. 12, no. 4, p. 174,
2008, doi: 10.1186/cc6975.

[19]   S. Mansouri, T. Alhadidi, S. Chabchoub, and R. B. Salah, "Impedance
cardiography: recent applications and developments," *Biomed. Res.*, vol. 29, no. 19,
2018, doi: 10.4066/biomedicalresearch.29-17-3479.

[20]   "Hemodynamic | SpringerLink."
https://link.springer.com/referenceworkentry/10.1007%2F978-1-4419-1005-9_1267
(accessed May 14, 2021).

[21]   V. Thanachartwet *et al.*, "Dynamic Measurement of Hemodynamic Parameters and Cardiac Preload in Adults with Dengue: A Prospective Observational Study," *PLoS ONE*, vol. 11, no. 5, May 2016, doi: 10.1371/journal.pone.0156135.

[22]   B. B. Hafen and S. Sharma, "Oxygen Saturation," in *StatPearls*, Treasure Island (FL): StatPearls Publishing, 2021. Accessed: May 14, 2021. [Online]. Available: http://www.ncbi.nlm.nih.gov/books/NBK525974/

[23]   "What is Oxygen Saturation?," *News-Medical.net*, Jun. 18, 2020. https://www.news-medical.net/health/What-is-Oxygen-Saturation.aspx (accessed Mar. 16, 2021).

[24]   "Bioimpedance is the method behind many medical diagnostic devices." https://www.eliko.ee/bioimpedance-medical-devices/ (accessed May 16, 2021).

[25]   A. Kasemaa, T. Rang, and P. Annus, "Analog Front End Components for Bio-Impedance Measurement: Current Source Design and Implementation," Jun. 2011, Accessed: May 16, 2021. [Online]. Available: https://digikogu.taltech.ee/et/Item/d25c72af-5586-4fb5-8321-36947dc9ccba

[26]   S. F. Khalil, M. S. Mohktar, and F. Ibrahim, "The Theory and Fundamentals of Bioimpedance Analysis in Clinical Status Monitoring and Diagnosis of Diseases," *Sensors*, vol. 14, no. 6, pp. 10895–10928, Jun. 2014, doi: 10.3390/s140610895.

[27]   "Fundamentals, Recent Advances, and Future Challenges in Bioimpedance Devices for Healthcare Applications." https://www.hindawi.com/journals/js/2019/9210258/ (accessed May 16, 2021).

[28]   J. Malmivuo and R. Plonsey, "Bioelectromagnetism. 25. Impedance Plethysmography," 1995, pp. 405–419.

[29]   V. address F. Sæl, s vei 24 0371 O. N. M. address P. O. box 1048 B. 0316 O. N. Phone, and fax, "What is bioimpedance? - Department of Physics." https://www.mn.uio.no/fysikk/english/research/projects/bioimpedance/whatis/index.html (accessed May 15, 2021).

[30]   A. R. A. Rahman, C.-M. Lo, and S. Bhansali, "A micro-electrode array biosensor for impedance spectroscopy of human umbilical vein endothelial cells," *Sens. Actuators B Chem.*, vol. 118, no. 1, pp. 115–120, Oct. 2006, doi: 10.1016/j.snb.2006.04.060.

[31]   K. S. Cole, *Membranes, Ions and Impulses: A Chapter of Classical Biophysics*. University of California Press, 1972.

[32]   T. K. Bera, "Bioelectrical Impedance and The Frequency Dependent Current Conduction Through Biological Tissues: A Short Review," *IOP Conf. Ser. Mater. Sci. Eng.*, vol. 331, p. 012005, Mar. 2018, doi: 10.1088/1757-899X/331/1/012005.

[33]   P. Batra and R. Kapoor, "Electrical Bioimpedance: Methods and Applications," vol. 3, no. 4, p. 6, 2015.

[34]   C. Aliau-Bonet and R. Pallas-Areny, "On the Effect of Body Capacitance to Ground in Tetrapolar Bioimpedance Measurements," *IEEE Trans. Biomed. Eng.*, vol. 59, Aug. 2012, doi: 10.1109/TBME.2012.2216880.

[35]   "Electrical Bioimpedance Measurement | Zurich Instruments." https://www.zhinst.com/europe/ko/applications/impedance-measurements/electrical-bioimpedance-measurement (accessed May 17, 2021).

[36]   E. Priidel, P. Annus, M. Metshein, R. Land, O. Märtens, and M. Min, "Lock-in integration for detection of tiny bioimpedance variations," in *2018 16th Biennial Baltic Electronics Conference (BEC)*, Oct. 2018, pp. 1–4. doi: 10.1109/BEC.2018.8600965.

[37]   T. K. Bera, "Bioelectrical Impedance Methods for Noninvasive Health Monitoring: A Review," *J. Med. Eng.*, vol. 2014, p. e381251, Jun. 2014, doi: 10.1155/2014/381251.

[38]   J. He, M. Wang, X. Li, G. Li, and L. Lin, "Pulse wave detection method based on the bio-impedance of the wrist," *Rev. Sci. Instrum.*, vol. 87, no. 5, p. 055001, May 2016, doi: 10.1063/1.4947514.

[39]   N. De Pinho Ferreira, C. Gehin, and B. Massot, "A Review of Methods for Non-Invasive Heart Rate Measurement on Wrist," *IRBM*, vol. 42, no. 1, pp. 4–18, Feb. 2021, doi: 10.1016/j.irbm.2020.04.001.

[40]   E. Priidel *et al.*, "Methods for Detection of Bioimpedance Variations in Resource Constrained Environments," *Sensors*, vol. 20, no. 5, Art. no. 5, Jan. 2020, doi: 10.3390/s20051363.

[41]   S. Hong, Y. Zhou, J. Shang, C. Xiao, and J. Sun, "Opportunities and challenges of deep learning methods for electrocardiogram data: A systematic review," *Comput. Biol. Med.*, vol. 122, p. 103801, Jul. 2020, doi: 10.1016/j.compbiomed.2020.103801.

[42]   G. Nikolic, R. L. Bishop, and J. B. Singh, "Sudden death recorded during Holter monitoring," *Circulation*, vol. 66, no. 1, pp. 218–225, 1982, doi: 10.1161/01.CIR.66.1.218.

[43]   "Holter monitor - Mayo Clinic." https://www.mayoclinic.org/tests-procedures/holter-monitor/about/pac-20385039 (accessed May 12, 2021).

[44]   D. T. Weiler, S. O. Villajuan, L. Edkins, S. Cleary, and J. J. Saleem, "Wearable Heart Rate Monitor Technology Accuracy in Research: A Comparative Study Between PPG and ECG Technology," *Proc. Hum. Factors Ergon. Soc. Annu. Meet.*, vol. 61, no. 1, pp. 1292–1296, Sep. 2017, doi: 10.1177/1541931213601804.

[45]   "ADUCM350: 16-Bit Precision, Low Power Meter on a Chip with Cortex-M3 and Connectivity | Design Center | Analog Devices." https://www.analog.com/en/design-center/landing-pages/001/aducm350-design-resources.html (accessed Apr. 11, 2021).

[46]   "ADUCM350 Datasheet and Product Info | Analog Devices." https://www.analog.com/en/products/aducm350.html?doc=EVAL-ADuCM350EBZ_UG-668.pdf#product-overview (accessed Apr. 11, 2021).

[55]   „14-Bit, 2-MSPS, Dual-Channel, Differential/Single-Ended, Ultralow-Power ADCs datasheet (Rev. B)" https://www.ti.com/lit/ds/symlink/ads7946.pdf?ts=1621325255067&ref_url=https%253A%252F%252Fwww.ti.com%252Fproduct%252FADS7946 (accessed Apr. 19, 2021).

[56]   „World's Lowest Power 9-Axis MEMS MotionTracking™ Device " https://invensense.tdk.com/wp-content/uploads/2016/06/DS-000189-ICM-20948-v1.3.pdf (accessed Apr. 19, 2021).

[57]   „Micron Serial NOR Flash Memory" MT25QU256ABA datasheet (datasheetspdf.com) (accessed Apr. 23, 2021).

[58]   „Maxim Integrated MAX30101 Pulse Oximeter & Heart-Rate Sensor" MAX30101 Pulse Oximeter & Heart-Rate Sensor - Maxim | Mouser (accessed Apr. 23, 2021).

APPENDICES 1 contains the functional code

Main C

/* Apply ADI MISRA Suppressions */

#define ASSERT_ADI_MISRA_SUPPRESSIONS

#include "misra.h"

#include <stddef.h>   /* for 'NULL' */

#include <string.h>   /* for strlen */

#include "spi.h"

#include "gpio.h"

#include "lib_aci.h"

#include "aci_setup.h"

#include "uart_over_ble.h"

#include "services.h"

extern int32_t adi_initpinmux(void);

extern void ftdi(void);

void spiTest(ADI_SPI_DEV_ID_TYPE const devID);

typedef struct {

   ADI_GPIO_PORT_TYPE Port;

   ADI_GPIO_DATA_TYPE Pins;

} PinMap;

PinMap MISO = {ADI_GPIO_PORT_3, ADI_GPIO_SPI0MISO};

```
PinMap MOSI = {ADI_GPIO_PORT_3, ADI_GPIO_SPI0MOSI};

PinMap SCLK = {ADI_GPIO_PORT_3, ADI_GPIO_SPI0SCLK};

PinMap RDYN = {ADI_GPIO_PORT_0, ADI_GPIO_P01};

PinMap REQN = {ADI_GPIO_PORT_2, ADI_GPIO_P214};

PinMap RESET = {ADI_GPIO_PORT_0, ADI_GPIO_P02};

#define NRF8001_SPI              ADI_SPI_DEVID_0

#define SPI_COMMON_PORT ADI_GPIO_PORT_3

#define RESET_GPIO_PORT ADI_GPIO_PORT_0

#define RDYN_GPIO_PORT  ADI_GPIO_PORT_0

#define REQN_GPIO_PORT  ADI_GPIO_PORT_2

#define RST_LOW       GPIO_ResetBits(RESET_GPIO_PORT, RESET_PIN)

#define RST_HIGH      GPIO_SetBits(RESET_GPIO_PORT, RESET_PIN)

#define REQN_LOW        GPIO_ResetBits(REQN_GPIO_PORT, REQN_PIN)

#define REQN_HIGH       GPIO_SetBits(REQN_GPIO_PORT, REQN_PIN)




#ifdef SERVICES_PIPE_TYPE_MAPPING_CONTENT

   static services_pipe_type_mapping_t

     services_pipe_type_mapping[NUMBER_OF_PIPES]                        =
SERVICES_PIPE_TYPE_MAPPING_CONTENT;

#else

   #define NUMBER_OF_PIPES 0
```

```c
    static services_pipe_type_mapping_t * services_pipe_type_mapping = NULL;

#endif

#define RXBUFFERSIZE   20

extern uint8_t Rx_Flag_read;

/* Store the setup for the nRF8001 in the flash of the AVR to save on RAM */

static      const      hal_aci_data_t      setup_msgs[NB_SETUP_MESSAGES]      =
SETUP_MESSAGES_CONTENT;

static struct aci_state_t aci_state;

/*

Temporary buffers for sending ACI commands

*/

static hal_aci_evt_t  aci_data;

//static hal_aci_data_t aci_cmd;



/*

Timing change state variable

*/

static bool timing_change_done         = false;

/*

Used to test the UART TX characteristic notification

*/

static uart_over_ble_t uart_over_ble;

uint8_t        uart_buffer[RXBUFFERSIZE];
```

```
static uint8_t        uart_buffer_len = 0;

static uint8_t        dummychar = 0;

bool stringComplete = false;  // whether the string is complete

uint8_t stringIndex = 0;

void nrf8001_setup()

{

 /**

  Point ACI data structures to the the setup data that the nRFgo studio generated for
the nRF8001

  */

 if (NULL != services_pipe_type_mapping)

 {

   aci_state.aci_setup_info.services_pipe_type_mapping                        =
&services_pipe_type_mapping[0];

 }

 else

 {

   aci_state.aci_setup_info.services_pipe_type_mapping = NULL;

 }

 aci_state.aci_setup_info.number_of_pipes    = NUMBER_OF_PIPES;

 aci_state.aci_setup_info.setup_msgs         = (hal_aci_data_t*)setup_msgs;

 aci_state.aci_setup_info.num_setup_msgs     = NB_SETUP_MESSAGES;

 /*

  Tell the ACI library, the MCU to nRF8001 pin connections.
```

The Active pin is optional and can be marked UNUSED

*/

aci_state.aci_pins.board_name   =   BOARD_DEFAULT;   //See   board.h   for   details
REDBEARLAB_SHIELD_V1_1 or BOARD_DEFAULT

aci_state.aci_pins.reqn_pin   =   REQN.Pins;   //SS   for   Nordic   board,   9   for
REDBEARLAB_SHIELD_V1_1

aci_state.aci_pins.rdyn_pin   =   RDYN.Pins;   //3   for   Nordic   board,   8   for
REDBEARLAB_SHIELD_V1_1

aci_state.aci_pins.mosi_pin   = MOSI.Pins;

aci_state.aci_pins.miso_pin   = MISO.Pins;

aci_state.aci_pins.sck_pin   = SCLK.Pins;

//aci_state.aci_pins.spi_clock_divider   = SPI_CLOCK_DIV8;//SPI_CLOCK_DIV8   =
2MHz SPI speed

//SPI_CLOCK_DIV16 = 1MHz SPI speed

aci_state.aci_pins.reset_pin   = RESET.Pins; //4 for Nordic board, UNUSED for
REDBEARLAB_SHIELD_V1_1

aci_state.aci_pins.active_pin   = UNUSED;

aci_state.aci_pins.optional_chip_sel_pin = UNUSED;

aci_state.aci_pins.interface_is_interrupt = false; //Interrupts still not available in
Chipkit

aci_state.aci_pins.interrupt_number   = 1;

//We reset the nRF8001 here by toggling the RESET line connected to the nRF8001

//If the RESET line is not available we call the ACI Radio Reset to soft reset the
nRF8001

//then we initialize the data structures required to setup the nRF8001

```c
    //The second parameter is for turning debug printing on for the ACI Commands and Events so they be printed on the Serial

  lib_aci_init(&aci_state, false);

}

void uart_over_ble_init(void)

{

  uart_over_ble.uart_rts_local = true;

}

bool uart_tx(uint8_t *buffer, uint8_t buffer_len)

{

  bool status = false;

  if (lib_aci_is_pipe_available(&aci_state, PIPE_UART_OVER_BTLE_UART_TX_TX) &&

     (aci_state.data_credit_available >= 1))

   {

    status   =   lib_aci_send_data(PIPE_UART_OVER_BTLE_UART_TX_TX,   buffer, buffer_len);

    if (status)

    {

     aci_state.data_credit_available--;

    }

   }


  return status;

}
```

```c
bool uart_process_control_point_rx(uint8_t *byte, uint8_t length)

{

  bool status = false;

  aci_ll_conn_params_t *conn_params;



  if                                           (lib_aci_is_pipe_available(&aci_state,
PIPE_UART_OVER_BTLE_UART_CONTROL_POINT_TX) )

  {

    printf("%02X\r\n", *byte);



    switch(*byte)

    {

      /*

      Queues a ACI Disconnect to the nRF8001 when this packet is received.

      May cause some of the UART packets being sent to be dropped

      */

      case UART_OVER_BLE_DISCONNECT:

        /*

        Parameters:

        None

        */

        lib_aci_disconnect(&aci_state, ACI_REASON_TERMINATE);
```

```
        status = true;

      break;



    /*

    Queues an ACI Change Timing to the nRF8001

    */

    case UART_OVER_BLE_LINK_TIMING_REQ:

      /*

      Parameters:

      Connection interval min: 2 bytes

      Connection interval max: 2 bytes

      Slave latency:         2 bytes

      Timeout:               2 bytes

      Same format as Peripheral Preferred Connection Parameters (See nRFgo studio -
> nRF8001 Configuration -> GAP Settings

      Refer to the ACI Change Timing Request in the nRF8001 Product Specifications

      */

      conn_params = (aci_ll_conn_params_t *)(byte+1);

      lib_aci_change_timing( conn_params->min_conn_interval,

                             conn_params->max_conn_interval,

                             conn_params->slave_latency,

                             conn_params->timeout_mult);
```

```c
    status = true;

    break;



/*

Clears the RTS of the UART over BLE

*/

case UART_OVER_BLE_TRANSMIT_STOP:

  /*

  Parameters:

  None

  */

  uart_over_ble.uart_rts_local = false;

  status = true;

  break;



/*

Set the RTS of the UART over BLE

*/

case UART_OVER_BLE_TRANSMIT_OK:

  /*

  Parameters:

  None
```

```
        */

        uart_over_ble.uart_rts_local = true;

        status = true;

        break;

    }

  }


  return status;

}


void aci_loop()

{

  static bool setup_required = false;


  // We enter the if statement only when there is a ACI event available to be processed

  if (lib_aci_event_get(&aci_state, &aci_data))

  {

    aci_evt_t * aci_evt;

    aci_evt = &aci_data.evt;

    switch(aci_evt->evt_opcode)

    {

      /**

      As soon as you reset the nRF8001 you will get an ACI Device Started Event
```

```
        */

        case ACI_EVT_DEVICE_STARTED:

        {

          aci_state.data_credit_total = aci_evt->params.device_started.credit_available;

          switch(aci_evt->params.device_started.device_mode)

          {

            case ACI_DEVICE_SETUP:

              /**

              When the device is in the setup mode

              */

              printf("Evt Device Started: Setup");

              setup_required = true;

              break;

            case ACI_DEVICE_STANDBY:

              printf("Evt Device Started: Standby");

              //Looking for an iPhone by sending radio advertisements

              //When an iPhone connects to us we will get an ACI_EVT_CONNECTED event
from the nRF8001

              if (aci_evt->params.device_started.hw_error)

              {

                delay(20); //Handle the HW error event correctly.

              }

              else
```

```c
            {

                lib_aci_connect(0/* in seconds : 0 means forever */, 0x0050 /* advertising
interval 50ms*/);

                printf("Advertising started : Tap Connect on the nRF UART app");

            }

            break;

        }

    }

    break; //ACI Device Started Event

    case ACI_EVT_CMD_RSP:

      //If an ACI command response event comes with an error -> stop

      if (ACI_STATUS_SUCCESS != aci_evt->params.cmd_rsp.cmd_status)

      {

        //ACI ReadDynamicData and ACI WriteDynamicData will have status codes of

        //TRANSACTION_CONTINUE and TRANSACTION_COMPLETE

        //all other ACI commands will have status code of ACI_STATUS_SCUCCESS for
a successful command

        printf("ACI Command %02X\r\n", aci_evt->params.cmd_rsp.cmd_opcode);

        printf("Evt    Cmd    respone:    Status    %02X\r\n",    aci_evt-
>params.cmd_rsp.cmd_status);

      }

      if         (ACI_CMD_GET_DEVICE_VERSION          ==         aci_evt-
>params.cmd_rsp.cmd_opcode)

      {
```

```
        //Store the version and configuration information of the nRF8001 in the Hardware
Revision String Characteristic

        lib_aci_set_local_data(&aci_state,
PIPE_DEVICE_INFORMATION_HARDWARE_REVISION_STRING_SET,

        (uint8_t          *)&(aci_evt->params.cmd_rsp.params.get_device_version),
sizeof(aci_evt_cmd_rsp_params_get_device_version_t));

        }

        break;

    case ACI_EVT_CONNECTED:

        printf("Evt Connected");

        uart_over_ble_init();

        timing_change_done          = false;

        aci_state.data_credit_available = aci_state.data_credit_total;



        /*

        Get the device version of the nRF8001 and store it in the Hardware Revision String

        */

        lib_aci_device_version();

        break;

    case ACI_EVT_PIPE_STATUS:

        printf("Evt Pipe Status");

        if (lib_aci_is_pipe_available(&aci_state,  PIPE_UART_OVER_BTLE_UART_TX_TX)
&& (false == timing_change_done))

        {
```

```c
        lib_aci_change_timing_GAP_PPCP(); // change the timing on the link as specified
in the nRFgo studio -> nRF8001 conf. -> GAP.

                                // Used to increase or decrease bandwidth

        timing_change_done = true;

        char hello[]="Hello World, works";

        uart_tx((uint8_t *)&hello[0], strlen(hello));

        printf("Sending : %s", hello);

      }

      break;

    case ACI_EVT_TIMING:

      printf("Evt link connection interval changed");

      lib_aci_set_local_data(&aci_state,

                        PIPE_UART_OVER_BTLE_UART_LINK_TIMING_CURRENT_SET,

                        (uint8_t *)&(aci_evt->params.timing.conn_rf_interval), /* Byte
aligned */

PIPE_UART_OVER_BTLE_UART_LINK_TIMING_CURRENT_SET_MAX_SIZE);

      break;

    case ACI_EVT_DISCONNECTED:

      printf("Evt Disconnected/Advertising timed out");

      lib_aci_connect(0/* in seconds   : 0 means forever */, 0x0050 /* advertising
interval 50ms*/);

      printf("Advertising started. Tap Connect on the nRF UART app");

      break;

    case ACI_EVT_DATA_RECEIVED:
```

```
      printf("Pipe Number: ");

      printf("%d\r\n", aci_evt->params.data_received.rx_data.pipe_number);


      if          (PIPE_UART_OVER_BTLE_UART_RX_RX          ==          aci_evt-
>params.data_received.rx_data.pipe_number)

        {

          printf(" Data(Hex) : ");

          for(int i=0; i<aci_evt->len - 2; i++)

          {

            printf("%c", (char)aci_evt->params.data_received.rx_data.aci_data[i]);

            uart_buffer[i] = aci_evt->params.data_received.rx_data.aci_data[i];

            printf(" ");

          }

          uart_buffer_len = aci_evt->len - 2;

          printf("\r\n");

          if                                    (lib_aci_is_pipe_available(&aci_state,
PIPE_UART_OVER_BTLE_UART_TX_TX))

          {

            /*Do this to test the loopback otherwise comment it out*/

            if (!uart_tx(&uart_buffer[0], aci_evt->len - 2))

            {

              Serial.println(F("UART loopback failed"));

            }

            else
```

```
        {

          Serial.println(F("UART loopback OK"));

        }

      }

    }

    if     (PIPE_UART_OVER_BTLE_UART_CONTROL_POINT_RX     ==     aci_evt-
>params.data_received.rx_data.pipe_number)

      {

        uart_process_control_point_rx(&aci_evt-
>params.data_received.rx_data.aci_data[0], aci_evt->len - 2); //Subtract for Opcode
and Pipe number

      }

      break;

    case ACI_EVT_DATA_CREDIT:

      aci_state.data_credit_available  =  aci_state.data_credit_available  +  aci_evt-
>params.data_credit.credit;

      break;

    case ACI_EVT_PIPE_ERROR:

      //See the appendix in the nRF8001 Product Specication for details on the error
codes

      printf("ACI     Evt     Pipe     Error:     Pipe     #:     %d",     aci_evt-
>params.pipe_error.pipe_number);

      printf("Pipe Error Code: 0x%02X", aci_evt->params.pipe_error.error_code);

      //Increment the credit available as the data packet was not sent.

      //The pipe error also represents the Attribute protocol Error Response sent from
the peer and that should not be counted
```

```c
    //for the credit.

    if           (ACI_STATUS_ERROR_PEER_ATT_ERROR           !=           aci_evt-
>params.pipe_error.error_code)

    {

      aci_state.data_credit_available++;

    }

    break;

  case ACI_EVT_HW_ERROR:

    printf("HW error: %d\r\n", aci_evt->params.hw_error.line_num);

    for(uint8_t counter = 0; counter <= (aci_evt->len - 3); counter++)

    {

      printf("%c", (aci_evt->params.hw_error.file_name[counter]));

    }

    printf("\r\n");

    lib_aci_connect(0, 0x0050);

    printf("Advertising started. Tap Connect on the nRF UART app");

    break;

  }

 }

 else

 {

   // No event in the ACI Event queue and if there is no event in the ACI command
queue the arduino can go to sleep

   // Arduino can go to sleep now
```

```c
    // Wakeup from sleep from the RDYN line

  }

  /* setup_required is set to true when the device starts up and enters setup mode.

   * It indicates that do_aci_setup() should be called. The flag should be cleared if

   * do_aci_setup() returns ACI_STATUS_TRANSACTION_COMPLETE.

   */

  if(setup_required)

  {

    if (SETUP_SUCCESS == do_aci_setup(&aci_state))

    {

      setup_required = false;

    }

  }

}

void print_setup_messages()

{

  int i, k;

  for (i = 0; i < NB_SETUP_MESSAGES; i++) {

    printf("index: %02x\r\n", setup_msgs[i].status_byte);

    for (k = 0; k < HAL_ACI_MAX_LENGTH; k++) {

      printf("%02x:", setup_msgs[i].buffer[k]);

    }

    printf("\r\n");
```

```c
        }

    }

    int main(void) {

        static uint32_t main_count = 0;

        static uint32_t rx_count = 0;

        char buffer[40];

        /* Clock initialization */

        SystemInit();

        /* Use static pinmuxing */

        adi_initpinmux();

        /* Call the routine that will interface to the FT4222 */

        ftdi();

        print_setup_messages();

        log_info("millis_init passed\r\n");

        nrf8001_setup();

        log_info("nrf8001_setup passed\r\n");

        while(1) {

            if (Rx_Flag_read) {

                printf("Rx_Flag_read is high\r\n");

                rx_count++;

                stringComplete = true;

                Rx_Flag_read = 0;

                printf("Sending: %s\r\n", (char *)&uart_buffer[0]);
```

```
        uart_buffer_len = stringIndex + 1;

        uart_buffer_len = RXBUFFERSIZE;

        if  (!lib_aci_send_data(PIPE_UART_OVER_BTLE_UART_TX_TX,  uart_buffer,
uart_buffer_len))

        {

            printf("Serial input dropped");

        }

        // clear the uart_buffer:

        for (stringIndex = 0; stringIndex < 20; stringIndex++)

        {

            uart_buffer[stringIndex] = ' ';

        }

        // reset the flag and the index in order to receive more data

        stringIndex   = 0;

        stringComplete = false;

    }

    aci_loop();

  }

}
```